HHS Public Access

Author manuscript

Nanomedicine (Lond). Author manuscript; available in PMC 2016 August 01.

Published in final edited form as:

Nanomedicine (Lond). 2015 August ; 10(15): 2379–2404. doi:10.2217/nnm.15.67.

Antimicrobial photodynamic inactivation in nanomedicine: small light strides against bad bugs

Rui Yin[1,2,3], **Tanupriya Agrawal**[2,3], **Usman Khan**[2,3], **Gaurav K Gupta**[2,3], **Vikrant Rai**[4], **Ying-Ying Huang**[2,3], and **Michael R Hamblin**[2,3,5,*]

[1]Department of Dermatology, Southwest Hospital, Third Military Medical University, Chongqing 400038, China

[2]Wellman Center for Photomedicine, Massachusetts General Hospital, BAR414, 40 Blossom Street, Boston, MA 02114, USA

[3]Department of Dermatology, Harvard Medical School, Boston, MA 02115, USA

[4]Wilf Family Cardiovascular Research Institute, Division of Cardiology, Department of Medicine, Albert Einstein College of Medicine, Bronx, NY 10461, USA

[5]Harvard-MIT Division of Health Sciences & Technology, Cambridge, MA 02139, USA

Abstract

The relentless advance of drug-resistance among pathogenic microbes, mandates a search for alternative approaches that will not cause resistance. Photodynamic inactivation (PDI) involves the combination of nontoxic dyes with harmless visible light to produce reactive oxygen species that can selectively kill microbial cells. PDI can be broad-spectrum in nature and can also destroy microbial cells in biofilms. Many different kinds of nanoparticles have been studied to potentiate antimicrobial PDI by improving photosensitizer solubility, photochemistry, photophysics and targeting. This review will cover photocatalytic disinfection with titania nanoparticles, carbon nanomaterials (fullerenes, carbon nanotubes and graphene), liposomes and polymeric nanoparticles. Natural polymers (chitosan and cellulose), gold and silver plasmonic nanoparticles, mesoporous silica, magnetic and upconverting nanoparticles have all been used for PDI.

Keywords

bacteria; carbon nanomaterials; fungi; liposomes; photodynamic therapy; photoinactivation; photosensitizer; titania photocatalysis; upconversion

Together with vaccines and public health measures to control transmission of communicable diseases, antibiotics have helped to dramatically reduce mortality from infectious disease during the 20th century [1]. However, the continuing global challenge of pathogens such as

*Author for correspondence: Tel.: +1 161 7726 6182, Hamblin@helix.mgh.harvard.edu.

Financial & competing interests disclosure

The authors have no relevant affiliations or financial involvement with any organization or entity with a financial interest in or financial conflict with the subject matter or materials discussed in the manuscript.

No writing assistance was utilized in the production of this manuscript.

influenza, tuberculosis and malaria, as well as the emergence of human immunodeficiency virus, means that infectious disease remains an important problem [2]. The real value of antibiotics goes beyond simply preventing death and illness due to infection, in that antibiotics also permit the serious iatrogenic assault on the immune system that occurs in cancer treatment or in organ transplantation, where they have helped to keep surgical complication rates down [3]. Therefore, antibiotics are an extremely valuable resource across the whole spectrum of modern medicine [4]. However, multidrug-resistant (MDR) and pandrug-resistant bacterial strains and the related infections they cause, have become emerging threats to public health throughout the world [5]. These infections are associated with an approximately twofold higher death rate, and with considerably prolonged hospital stays [6]. Infections caused by antibiotic resistant microbes are often exceptionally hard to treat due to the limited range of therapeutic options [7]. Therefore, there is an urgent need for an all-out search for alternative antimicrobial approaches to kill MDR strains, concentrating on methods that are unlikely to cause resistance to develop [8–10]. Recently, Bush *et al.* pointed out that novel nonantibiotic approaches to prevent and treat infectious disease should be considered high-priority international research and development goals [11]. A promising, innovative approach to achieve this goal is antimicrobial photodynamic inactivation (aPDI).

Mechanisms of photodynamic therapy

The principles underlying aPDI or photodynamic therapy (PDT) are similar. Both techniques combine a nontoxic dye termed a photosensitizer (PS) and harmless low-intensity visible light of suitable wavelength to match the PS absorption peak. The mechanisms are graphically illustrated in Figure 1. The PS initially absorbs light to form the short-lived first excited singlet state. The excited singlet PS can undergo intersystem crossing to form the much longer-lived excited triplet state that can survive long enough to carry out chemical reactions. The triplet PS can react in the presence of ambient molecular oxygen to produce two types of photochemical reactions (type I and type II) [12]. Type I photoprocesses involve hydrogen or electron-transfer reactions between the excited state PS and other molecules in the environment (frequently oxygen). These electron-transfer reactions produce (directly or indirectly) reactive oxygen species (ROS) that are harmful to cells, such as superoxide ($O_2^{\bullet -}$), hydrogen peroxide (H_2O_2), hydroxyl radicals ($HO^{\bullet}$) and hydroperoxyl radicals ($HOO^{\bullet}$). The type II photoprocess is an energy transfer mechanism involving electron spin exchange between the excited triplet state PS and ground state oxygen ($^3O_2$), itself a triplet. Triplet-triplet interactions are spin-allowed, but singlet-triplet interactions are spin-forbidden, so the fact that ground state oxygen happens to be a triplet is important in this regard. Type I and type II reactions both produce ROS that cause oxidation of biomolecules (lipids, proteins and nucleic acids) in the cell. In the case of microbial cells most of the damage is carried out at the cell wall, and cells are permeabilized so that essential components such as nucleic acids leak out.

Antimicrobial PDI

There are two main classes of bacteria (Gram-positive and Gram-negative) defined by their response to the Gram stain, which reflects differences in their morphology as illustrated in

Figure 2. Numerous studies have shown that there is a fundamental difference in susceptibility to antibacterial PDI between Gram-positive and Gram-negative bacteria due to differences in the organization of the outer membrane structures [13–16].

The cell wall of Gram-positive bacteria is composed mainly of thick porous layers of peptidoglycan embedded with proteins and lipotechoic acid, which will allow PS to easily pass through [17]. Additionally the negatively charged lipotechoic acids on the outside contribute to binding of cationic agents [18,19]. By contrast, the cell wall of Gram-negative bacteria consists of a thin layer of peptidoglycan adjacent to the inner cytoplasmatic membrane as well as an outer membrane with phospholipids and negatively charged lipopolysaccarides that give Gram-negative species an even more pronounced negative charge than Gram-positive cells. This outer membrane provides an effective permeability barrier and limits the binding and penetration of anionic and lipophilic PS [19]. The effectiveness of aPDT against Gram-negative bacteria can be enhanced by combination with a permeabilizing agent (e.g., Tris-EDTA or polymyxin nonapeptide) to destabilize the lipopolysaccarides coating by removing the Ca^{2+} and Mg^{2+} ion [17,20,21].

However, direct PDI of Gram-negative bacteria is also possible. There are now many different positively charged PS with structures belonging to several chemical classes, including phthalocyanines and porphyrins, that have been successfully tested as photosensitizers against Gram-positive and Gram-negative bacteria [22–26]. Tetrapyrrole photosensitizers with an overall cationic charge such as mesosubstituted cationic porphyrins and water-soluble cationic zinc phthalocyanines can efficiently kill Gram-negative bacteria by aPDT action even in the absence of permeabilizing agents.

At present, there is a consensus that aPDI can inactivate all known classes of microorganism, including Gram-positive, Gram-negative bacteria, fungi, protozoa, viruses, etc., whether *in vitro* or *in vivo* [8,9,27]. Furthermore, aPDI is thought to be equally effective (or even more effective) against MDR species compared with naive species [28]. Moreover PDI treatment itself is unlikely to cause resistance, as damage by ROS is thought be via a nonspecific killing mechanisms compared with antibiotics that generally inhibit a specific enzyme [29,30]. PDI does not lead to the selection of mutant resistant strains which is another advantage compared with standard antibiotics [31].

There is some debate about whether the ROS that is generated outside the microbial cell can efficiently kill from the outside, or whether ROS that is generated inside the outer membrane is much more effective in killing. Both scenarios are almost certainly the case, and the construction and testing of photoactivated surfaces [32], films [33] and solid supported photosensitizers [34] has provided new applications in environmental aPDI.

The American Society of Microbiology has decreed that in order for any technology to claim to be ‘antimicrobial’ it has to kill more that 3 logs of planktonic cells. In many cases 6 or more logs of killing may be achieved that is frequently equivalent to eradication (no CFU remaining). When microbial cells are growing in biofilms they are considerably more resistant to PDI compared with to planktonic cells. In the case of biofilm growing cells 1 or 2 logs of inactivation may be considered biologically significant.

Nanoparticles & nanomedicine in PDT

Nanomedicine is defined as the medical application of nanotechnology for the diagnosis and treatment of human disease. It uses precisely engineered materials, known as nanoparticles, with dimensions generally in the 1–200-nm range. One of the most important functions of medical nanotechnology is as drug delivery vehicles that can improve drug availability at the target area to provide the maximum therapeutic benefit. Nanomaterials can improve the solubility of poorly water-soluble drugs, prolong the circulation time in the bloodstream, minimize the enzymatic degradation of the drug, decrease undesirable side effects and increase bioavailability. In the last decade, PDT has also been combined with nanotechnology techniques, as the photochemical effectiveness can be greatly enhanced by the use of nanoparticles. There are many aspects of PDT which can be improved, such as light dosimetry, when the use of high fluence rates of the exciting light can cause oxygen depletion and photosensitizer photobleaching [35], and optimization of the rate of production of singlet oxygen, when too little is inefficient and too much can result in normal tissue damage [36]. However, one of the most important problems to be overcome in PDT is optimizing drug delivery [37]. A key limitation in PDT is the poor water solubility of many PS, and their tendency to aggregate in the aqueous environment in physiological conditions. To improve PS delivery to the target tissue, it is possible to rationally design nanoagents as carriers and vehicles for drug delivery. Appropriately chosen nanoparticles can increase the solubility of hydrophobic PS, and additionally have the proper size to accumulate in the tumor via the enhanced permeability and retention effect caused by the immature tumor vaculature.

Different approaches have been investigated to combine nanoparticles and PDI, for antimicrobial applications. One use of nanoparticles is to improve the binding and uptake of PS by the microbial cells; while another use is to improve the microbial photoinactivation kinetics [31]. There are two basically different ways to use nanoparticles in PS delivery: covalent conjugation where a chemical bond is used to attach the PS to a constituent of the nanostructure as shown in Figure 3; noncovalent encapsulation or incorporation in various nanocontainers (Figure 4). PS can be modified by encapsulation in delivery agents such as liposomes [38], micelles [39–42], gold nanoparticles [43,44], polymer nanoparticles [45], ceramic-based nanoparticles [46] and carbon nanotubes [47]. Another possibility is to use nanodiamonds [48,49]. These structures are commercially available carbon nanomaterials with a diamond structure (sp3 hybridization) and have good biocompatibility and low cytotoxicity. They have the capability for controlled release of drugs, have a narrow particle size distribution, a high surface area to volume ratio and a high capacity for drug loading [48,49].

Photosensitizers can be modified by attaching them to dendrimers (Figure 3A). Dendrimers are highly complex molecules that are sequentially built up by a series of solution reactions. They possess a core, branches and end groups [51], which can be conjugated or loaded with PS molecules. Dendrimers can be constructed with different sizes and lipophilicity in order to optimize the uptake by cells, and can be designed to carry a high drug payload [52]. Unlike conventional PS, dendrimer-PS conjugates demonstrate good ROS production even at extremely high concentrations as the individual PS molecules are kept apart from each

other by the dendrimer framework so they cannot self-quench. Typical examples are ionic dendrimer PS conjugates where a core porphyrin or phthalocyanine has large dendritic wedges attached to the periphery, which sterically prevent aggregation of the central tetrapyrrole molecules [22].

Fullerenes have a molecular diameter at the lower end of the nanoparticle scale (Ø 1 nm), but they have very high photostability and produce a combination of both singlet oxygen (type 2) and also type I reactive oxygen species, such as superoxide or hydroxyl radicals. Appropriately functionalized fullerenes (with multiple attached cationic groups) have been shown to have good selectivity for binding to microbial cells compared with mammalian cells and have been studied in antimicrobial applications [30]. Rose Bengal is one of the most frequently used PS due to its ready availability, high water solubility, high singlet oxygen quantum yield and low rate of photodegradation [53], and has been attached to silica nanoparticles to inactivate Gram-positive bacteria, including methicillinresistant *Staphylococcus aureus* (MRSA) [54]. Related studies on methylene blue (a phenothiazinium dye) loaded nanoparticles have also been reported [55,56].

Titania photocatalysis

Photocatalysis is the acceleration of a light-mediated reaction in the presence of a catalyst (usually an inorganic semiconductor) [57]. Over the last 30 years there has been an increasing interest in the use of titanium dioxide (TiO_2) as a photocatalyst due to its highly efficient photocatalytic properties that allow destruction of organic polluting chemicals and also the killing of pathogenic microbes [58]. The advantage of photocatalysis is having sunlight or UV radiation to trigger the disinfection process using a catalyst (TiO_2) [23].

TiO_2 is a wide band-gap, n-type semiconductor, with the characteristics of low toxicity, strong optical absorption, low cost and high chemical stability. It has been used in photovoltaic, photodegradation, photocatalysis, electrochromic devices and so on. When TiO_2 nanoparticles are excited by UV light (λ <385 nm), photo-induced electrons and photogenerated charged holes are created (see Figure 5 for a schematic explanation). These electron-hole pairs are generated when TiO_2 absorbs the energy of the photons with sufficient energy (3.2 eV) (hν) to the band gap [24]. The energy difference between the valence band (e_{vb}^-) and the conduction band (e_{cb}^-) is known as the band gap.

The absorption of energy and the subsequent generation of the electron–hole pair are given by the following equation:

$$TiO_2 + h\nu \rightarrow e_{cb}^-(TiO_2) + h_{vb}^+(TiO_2)$$

where e− is the conduction band electron and *h*+ is the valence band hole. The reaction of the hole with surrounding water molecules and hydroxide ions produces the reactive hydroxyl radicals [25,59].

$$h_{vb}^+ + H_2O \rightarrow H^+ + OH^\bullet$$

The electrons react with molecular oxygen to form superoxide radical anions

$$e_{cb}^{-} + O_2 \rightarrow O_2^{\bullet -}$$

Highly reactive oxygen species such as hydroxyl radicals ($^{\bullet}OH$) serves as the main oxidant and is capable of killing a wide range of microorganisms, including bacteria, fungi, algae, protozoa and viruses (Tables 1–3).

The fact that the active form of TiO_2 is the nanoparticle form has allowed it to be incorporated into paints, films, and a host of different materials that can be made 'self-sterilizing.' A variety of medical applications of TiO_2 photocatalysis have been proposed, among which are self-sterilizing urinary catheters [93], self-sterilizing lancet for blood glucose determination [94], antibacterial food packaging film [95], antibacterial dental implants [96], antibacterial surgical implants [97] and many more.

Fullerenes

The fullerene molecule has a unique structure entirely composed of sp2 hybridized carbon atoms arranged in a soccer ball structure [98]. It was originally named as 'Buckminsterfullerene,' after the architect R Buckminster Fuller due to its structural similarity to his geodesic dome constructions [99]. Fullerenes and their derivatives have been a magnet for both scientific and industrial attention because of their ability to act as lubricants, their simple fabrication process and the prospect for low-cost production in a large-scale manufacturing process. They are widely accepted nanoparticles, and have been increasingly used in the field of nanotechnology especially in biomedical applications [100–102]. Their most important medical application is the light-based therapy PDT [103]. Fullerenes have certain particular advantages over more traditional PS based on tetrapyrrole and phenothiazinium backbones [104]. Fullerenes (and in particular soluble functionalized fullerenes) are able to act as PS in PDT/PDI, as the triplet state of the fullerene molecule has a very high triplet yield and a long triplet lifetime that can interact with molecular oxygen [105]. Their disadvantages lies in their absorption spectrum, which is inclined toward the blue and green visible wavelengths rather than the red/far red wavelengths that have good tissue penetration. Second, pristine fullerenes are difficult to be made water-soluble and have a marked tendency to aggregate. However, functionalized fullerenes can be made water soluble and are effective as antimicrobial PS in the treatment of relatively superficial infections (for instance, in wounds and burns), where the penetration depth of the light does not need to exceed more than 1.0 mm.

Recently, these functionalized fullerenes have been studied for their biological activities to mediate PDI in combating invasive microbial infections [30]. The chemical structures of the fullerenes discussed here are given in Figure 6. Previous work from our lab, has shown that the presence of one or more cationic charges can greatly increase the binding to the negatively charged microbial membranes, while the hydrophobic character then increases the penetration into the lipid components of the membrane [26,106]. A C60 fullerene functionalized with three dimethylpyrrolidinium groups (BF6) was found to be a highly active broad-spectrum antimicrobial photosensitizer able to kill Gram-positive bacteria,

Gram-negative bacteria and fungal yeast cells *in vitro* when combined with white-light illumination (4–6 logs) [106]. The performance of this compound was better than a widely used antimicrobial PS, toluidine Blue O.

Lu *et al.* were the first to report that mouse models of wounds infected with potentially lethal bacteria *Proteus mirabilis* and *Pseudomonas aeruginosa* could be cured of a fatal bacterial infection by aPDT mediated by BF6 and white light (Figure 6A) [107]. A synergistic effect of antimicrobial PDT with traditional antibiotics was also reported for the first time [107]. Mizuno *et al.* showed that fullerenes that carry more cationic groups are more effective broad-spectrum antimicrobial PS [103], and showed the most effective compounds had more cationic charges and a lower logP value [30]. These workers also compared a new group of synthetic fullerene derivatives that possessed either basic amino groups or quaternary ammonium groups as antimicrobial PS against Gram-positive (*Staphylococcus aureus*), Gram-negative bacteria (*Escherichia coli*) and fungi (*Candida albicans*). The nonquaternary amino groups tended to form nanoaggregates in water and were only effective against Gram-positive *S. aureus*. An increase in the number of quaternary cationic groups tended to minimize aggregation, and a compound with six quaternary N-atoms was found to be most effective compound giving up to 6 logs of killing. *S. aureus* was most susceptible; *E. coli* was intermediate, while *C. albicans* was the most resistant species tested [103].

Huang *et al.* [108] investigated water soluble decacationic fullerene monoadducts, C60[>M($C_3N_6^+C_3$)$_2$] and C70[>M($C_3N_6^+C_3$)$_2$], for photodynamic inactivation of Gram-positive (e.g., *S. aureus*) and Gram-negative (e.g., *E. coli*). More than six logs of each species were killed by illumination with white light using the most effective compound. The compound C70[>M($C_3N_6^+C_3$)$_2$] possessing a higher number of electron-donating iodide anions produced more highly reactive HO• radicals and singlet oxygen ($^1O_2$) than compound C60[>M($C_3N_6^+C_3$)$_2$]. These results explained the killing of Gram-positive and Gram-negative bacteria by C60[>M($C_3N_6^+C_3$)$_2$](Figure 6B) and C70[>M($C_3N_6^+C_3$)$_2$] (Figure 6C). In Gram-positive bacteria $^1O_2$ can diffuse more easily into porous cell walls whereas in Gram-negative bacteria the cell wall is less permeable so the more reactive HO$^\bullet$ is required to cause real damage and bacterial killing [108].

Wang *et al.* reported a unique class of water-soluble fullerene adducts, decacationic methano [95] fullerene decaiodides C60[>M($C_3N_6^+C_3$)$_2$]-(I^-)$_{10}$ [1-(I^-)$_{10}$]. These compounds when excited with both UVA light and white light was capable of generating $^1O_2$ (type-II) and also highly reactive hydroxyl radicals formed from superoxide, via a type-I photochemical reaction [109,110]. The ten quaternary ammonium cationic charges per C60 cage was designed to boost the ability of the fullerene to target Gram-positive (>6 logs of killing) and Gram-negative bacteria (2.5 logs of killing) using white light [109].

A recent study, used a [C60]-fullerene and its derivative that were immobilized onto a polymer support, macroporous silicone (dimethylsiloxane), to carry out inactivation of waterborne bacteria (*Enterococcus faecalis*) [111]. Favorable absorption of visible light, and high ROS quantum yields of silicone-embedded C60-fullerene were noted, but it was still found to be inferior in photodynamic water disinfection compared with Ru(II) polypyridyls

immobilized onto the same support [111]. The light-mediated antimicrobial activities of fullerene C60 and its derivatives were studied by Aoshima *et al.* against both bacteria and fungi [112]. They used water-soluble fullerenes encapsulated into carriers (polyvinylpyrrolidone (PVP)/C60, gammacyclodextrin (gamma-CD)/C_{60}, and nano-C_{60}) and 3 types of fullerenols ($C_{60}(OH)_{12}$, $C_{60}(OH)_{36}{\cdot}8H_2O$, and $C_{60}(OH)_{44}{\cdot}8H_2O$). The fullerenols displayed good antimicrobial activity against *Propionibacterium acnes, Staphylococcus epidermidis, C. albicans* and *Malassezia furfur*. Additionally, the study found that the activity of fullerenols against fungi was stronger than against bacteria. This finding was explained by the authors who pointed out the fact that fullerenols are more water soluble and could interact more with components such as β-glucan and chitin in fungus cell-wall than with peptidoglycan in the bacterial cell membrane [112].

Carbon nanotubes

In 1991 the Japanese scientist, Sumio Iijima first reported the discovery of carbon nanotubes (CNTs) as a by-product of fullerene synthesis [113]. Remarkable progress has been made since, including the discovery of two basic types of nanotubes: multiwalled, referred to as (MWNT and MWCNT) and single-walled, referred to as (SWNT and SWCNT) (Figure 7) [114]. CNTs have a high aspect ratio (length to diameter) and a large surface area relative to their molecular weight, have been suggested as potential candidates for industrial use in areas such as hydrogen storage [115] and agents to remove contaminants from water and air [116]. The excellent mechanical properties of CNT are due to the strength of the sp^2 carbon–carbon bonds. CNTs cluster naturally into nanoropes held together by weak van der Waals forces. Depending on their fine structure CNT can behave as 1D quantum wires composed entirely of carbon (metallic form) or as semiconductors. The walls of the SWCNT are one atom thick and tens of atoms in circumference. Every carbon atom composes the surface of the nanotube and contributes to covalent bonds. SWNTs are typically about 1 nm in diameter but could be hundreds of nanometer to several centimeter long. These properties, coupled with the lightness give CNT their great potential in many biological applications [114]. MWNTs are also potent antiviral agents.

Using layer-by-layer assembly, Nepal *et al.* created SWNTs coated with the antimicrobial molecule, lysozyme [117], which has strong antibacterial properties against Gram-positive bacteria. The study showed that a coating of lysozyme on SWNTs had significant effects against *Micrococcus lysodeikticus* and *S. aureus* [118]. Porphyrin-conjugated MWNTs excited by visible light were found to significantly reduce the ability of influenza A virus to infect mammalian cells. This finding could lead to development of other MWNTs for antiviral therapeutics [119]. A novel report in 2013 showed that MWCNT arrays could be used for deposition of TiO_2 nanoparticles resulting in removal of the pathogen, enterohemorrhagic *E. coli* O157:H7 (EHEC) (see Figure 8) [120]. The vertical array of MWCNT acted as a filter for bacterial retention, while TiO_2 acted as an efficient bactericidal photocatalyst. The deadly EHEC was filtered through TiO_2/MWCNT coated porous ceramic filter and bacterial removal was found to be significantly lower. The authors hypothesized that the photo-generated electrons in MWCNT might react with the dissolved oxygen molecules, thus producing superoxide radicals $O_2^{\bullet-}$. Holes generated in TiO_2 nanoparticles may react with the OH^- which is obtained from water molecules to form hydroxyl radicals

$OH^{\bullet}$. *E. coli* O157:H7 can then be photocatalytically killed by both $O_2^{\bullet-}$ and $HO^{\bullet}$ (Figure 8) using UVA light. Dinu *et al.* combined peracetic acid (PAA) with MWNT to produce bioactive composites that acted as a potent oxidizing agent that could be used for disinfection, with broad effectiveness against bacteria, yeasts, fungi and spores. They were able to successfully kill more than 99% of spores initially present at 10^6 CFU/ml [121].

Graphene

Graphene is a 2D sheet of sp2 and sp3 hybridized carbon atoms. It is the simplest of the carbon nanostructures having structural features in common with fullerenes (3D closed cage), carbon nanotubes (3D rolled tube) and graphite (3D stack of sheets). Graphene has a single atom thin, 2D honeycomb lattice and the carbon atoms also include carboxyl, hydroxyl and epoxide functional groups [122]. Graphene oxide (GO), a water-soluble derivative, has excellent biocompatibility, stability in aqueous medium, large specific surface area that can be loaded with huge quantities of hydrophobic drugs such as doxorubicin. It has attracted great interest from scientists [123,124] due to its abilities to solubilize hydrophobic molecules between the sheets due to π–π stacking (Figure 9A). Graphene and graphene oxide sheets can also be used to solubilize hydrophobic PS such as 2-(1-hexyloxyethyl)-2-devinyl pyropheophorbide-alpha (HPPH or Photochlor®; Figure 9B) [125], hypocrellin A (Figure 9C) [126] and methylene blue (Figure 9D) [127]. In a recent study, electrochemically produced graphene quantum dots (GQD), when photoexcited with a green laser (470 nm, 1 W), were found to generate ROS and kill two strains of bacteria, MRSA and *E. coli* but were ineffective in killing mouse spleen cells demonstrating a legitimately selective antibacterial photodynamic action of GQD [128]. Another group [129] suggested the application of GQD combined with low levels of H_2O_2 to produce 'antibacterial band aids' for wound disinfection. The peroxidase-like activity of the GQD produced $HO^{\bullet}$ from H_2O_2, and the effectiveness of the bandage was demonstrated in wound infections in mice.

Liposomes

Liposomes are spherical nanosized vesicles made from a self-assemble lipid bilayer formed from natural phospholipids and cholesterol. Since the discovery of liposomes in 1961 by Alec D Bangham, they have become a very useful tool in biology, biochemistry and medicine [130,131]. Liposomes are the most extensively studied colloidal carrier system, that can be loaded with substances such as drugs and PS with the goal to solubilize, deliver and transport them to a specific target, thus preventing the drug from degradation as well as limiting adverse effects from nontargeted drug [131]. Liposomes are primarily made of one or more concentric phospholipid bilayers each unit of which consists of an inner hydrophilic head and outer hydrophilic tail. The hydrophobic center of these bilayers can accommodate hydrophobic drugs or PS, while the hydrophilic central region or core can accommodate water-soluble drugs or PS [132,133]. PS can therefore be encapsulated into liposomes depending on the lipophilicity and water solubility of the PS itself (Figure 3D & 4D). After the PS is packed in the liposome there are two mechanisms of uptake by the cells: either the liposomes undergo fusion with the cell membrane and release the contents into the cytosol, or phagocytic cells can engulf these liposomes and disintegrate them inside the endosomes

or lysosomes, thereby releasing the active drug into the cell [134]. Studies have suggested that PS administered using liposomes can substantially improve the efficacy and safety of PDT/PDI. The efficacy of antimicrobial PDI can also be increased by loading the PS into biocompatible liposomes [135–138].

Liposomes formed from N-(1-[2,3-dioleoyloxy] propyl)-N,N,N-trimethylammonium chloride were used as carriers loaded with a positively charged meso-substituted porphyrin, namely 5-(4-[1-dodecanoylpyridinium])-10,15,20-triphenylporphyrin (Figure 10A). The liposomal carrier disorganized the native structure of the bacterial cell wall, and enhanced the ability of the PS to pass through, leading to a deeper penetration of the drug into the plasma membrane, and to more cell death (up to 6 logs) on white light illumination [139].

Bombelli *et al.* improved the antibacterial activity of the PS m-tetrahydroxyphenylchlorin (temoporfin, Figure 10B), by encapsulating it in a cationic liposome preparation composed of different ratios of dimyristoyl-sn-glycero-phosphatidylcholine (DMPC) combined with any of four cationic surfactants (CS): (1S,2S)-N-hexadecyl-N-methylprolinolinium bromide, (1R,2S)-N-hexadecyl-Nmethylprolinolinium bromide, N-hexadecyl-L-prolinoliniumhydrobromide and 3-N,N-dihexadecyl-l-prolinoliniumbromide. This cationic liposomal-delivered temoporfin preparation was evaluated against MRSA, and one of these formulations had the same bactericidal activity as free temoporfin [140].

Although cetyltrimethyl ammonium bromide (CTAB) demonstrates strong intrinsic antimicrobial activity due to its amphiphilic properties, CTAB also exhibits high affinity toward biological membranes of host cells, rendering it unsuitable for direct use as an antimicrobial [141]. Recently, Yang *et al.* incorporated CTAB into the lipid bilayer of dimyristoyl-sn-glycero-phosphatidylcholine (DMPC) liposomes into which chlorin(e6) (Ce6; Figure 10C) was also encapsulated. They tested the *in vitro* PDI efficacy of this preparation against susceptible and drug-resistant clinical isolates of *C. albicans* as well as in infected burn wounds [142]. This liposomal formulation showed enhanced PDI efficacy against both susceptible and clinical drug-resistant strains of *C. albicans* demonstrating that microbial outer-wall disruption can be accomplished by using positively-charged liposomes encapsulating hydrophobic photosensitizers [142]. The main disadvantage of these cationic liposomes could be that in infected tissue the PS is delivered not only to the bacterial cell wall but also to the surrounding cells. Cationic liposomes easily fuse with host cells as the mammalian cell membrane is negatively charged, and there could be side effects with light [142]. To overcome this disadvantage of cationic liposomes, Yang *et al.* conjugated a novel antimicrobial peptide (WLBU2) to the surface of potent second-generation PS, temoporfin-loaded liposomes [143]. Subsequently, the WLBU2-modified liposomes photo-eradicated all MRSA and induced a greater than 3 log(10) reduction of *P. aeruginosa in vitro* confirming enhanced temoporfin delivery to bacteria [143].

One of the major issues with PDT is the limited tissue penetration of external light delivered from conventional light sources [144]. Because of this aPDT is considered to be restricted to superficial infections and has very limited use against deep infections. Previous studies have shown that cancer cells could be destroyed using intracellular chemiluminescence as the light source to excite a PS [145,146]. On the basis of these studies, Nakonechny *et al.*,

exploited light emitted as a result of the internal chemiluminescent reaction of luminol to excite the PS and named the process 'chemiluminescent photodynamic antimicrobial therapy' (CPAT) [147]. The antibacterial effect of free and liposome-encapsulated PS (methylene blue or toluidine blue) excited by both white external light and by chemiluminescence mediated by free or liposome-enclosed luminol was studied. The efficacy of PDI using external light showed slightly higher killing than liposome-enclosed luminol and both free and encapsulated PS against both types of bacteria. However, CPAT showed a higher efficacy in killing and inhibiting the growth of both Gram-positive (*S. aureus* 3 log) and Gram-negative bacteria (*E. coli* 2 log) [147]. CPAT allows PDI in the absence of a conventional light source to activate the PS, and may be effective for deep infections that are difficult to treat using traditional PDI.

Polymeric nanoparticles

Polymeric nanoparticles possess advantages compared with other nanodelivery vehicles. The drug is entrapped, encapsulated or attached to a nanoparticle matrix and depending upon the method of preparation, nanoparticles, nanospheres or nanocapsules can be obtained. Nanocapsules are containers in which the drug is contained in a cavity surrounded by a polymer membrane, while nanospheres are matrix systems with the drug uniformly dispersed throughout the nanoparticle [50]. Biodegradable polymeric nanoparticles have been used as drug delivery vehicles for controlled release of many drugs. They are also able to target particular organs/tissues as carriers of DNA in gene therapy, and to deliver proteins, peptides and genes through oral administration because they protect their cargo from degradation in the stomach [148,149].

Hypericin (HY; Figure 10D) is a naturally-occurring compound isolated from St Johns Wort that acts as a potent photosensitizer [150]. However its lipophilicity and its tendency to aggregate in an aqueous environment limits its therapeutic applications. Nafee *et al.* developed a biodegradable nanocarrier for hypericin that allowed it to function as an antibacterial photosensitizer [151]. Hypericin-loaded nanoparticles (HY-NPs) were prepared from amphiphilic block copolymers. The antimicrobial photoactivity of HY-NPs was tested *in vitro* against MRSA clinical isolates as both planktonic and biofilm-embedded cells, and *in vivo* against infected wounds in rats. Light-activated HY-NPs demonstrated better inhibition of biofilm cells compared with planktonic cells. *In vivo* wound healing studies in rats revealed better epithelialization and quicker wound healing, accompanied by increased keratinization and growth of collagen fibers when light-activated HY-NPs were used.

Antibacterial nanoparticles to improve root canal disinfection have also been investigated. A study by Pagonis *et al.* examined the *in vitro* effects of a biodegradable preparation of poly(lactic-co-glycolic acid) nanoparticles loaded with the PS methylene blue (MB, Figure 10E) using PDI to kill *E. faecalis* [152]. Methylene blue (MB) (a well-established photosensitizer) was used to kill various Gram-positive and Gram-negative oral bacteria [153]. The interaction of light activated PDI and MB-loaded nanoparticles led to approximately 2 log10 reduction of CFU in planktonic cells, and a 1 log10 reduction in CFU in root canal biofilms.

Chitosan

Chitosan (CS; Figure 11A) is a polycationic polymer composed of N-acetyl-d-glucosamine and b-1,4-linked D-glucosamine. It is derived by partial deacetylation of chitin, the structural material of arthropod shells. The polycationic nature of CS interferes with the negatively charged residues of macromolecules at the microbial cell surface, which explains its ability to potentiate PDI using many different PS [154,155]. Due to its safety combined with excellent biocompatibility and biodegradability, CS has been extensively explored for medical applications in wound healing [156,157], tissue engineering [158] and drug delivery [159]. CS has a pKa value of approximately 6.3 [160]. Therefore at low pH values, CS is cationic due to the protonation of the amino groups. CS nanoparticles can be readily prepared by ionic gelation, a process involving cross-linking of the cationic CS with inorganic polyanions, such as sodium tripolyphosphate. The formulation of these nanoparticles occurs spontaneously upon addition of the counter-anion sodium tripolyphosphate into a CS solution without heat or organic solvents [161].

Rose Bengal (Figure 10F) delivered by functionalized bioactive polymeric chitosan nanoparticles, CSRBnp were shown to produce antibiofilm effects. Photoactivated CSRBnp resulted in reduced viability of *E. faecalis* biofilms and disruption of biofilm structure, leading to efficient elimination of bacterial-biofilms and stabilization of dentin-matrix [162]. CSRBnp also showed significant antibacterial efficacy and completely eliminated the bacteria after 24 h of interaction after photodynamic therapy, even in the presence of tissue components, such as dentin, dentin-matrix, pulp tissue, bacterial lipopolysaccharide and protein (bovine serum albumin) that are present within root canals [162]. Polycationic chitosan-conjugated RB demonstrated photoinactivation of biofilms of *E. faecalis* (Gram-positive) and *P. aeruginosa* (Gram-negative), resulting in significantly higher elimination than RB and MB excited in the free form [163]. Erythrosine (ER) combined with CS nanoparticles and exposed to light showed significant phototoxicity to the planktonic cells and biofilms of *Streptococcus mutans, P. aeruginosa* and *C. albicans.* The antimicrobial activity of ER/CS nanoparticles was again significantly higher than that of ER in the free form [164]. Chitosan nanoparticles loaded with methylene blue also showed a large synergistic potentiation of photodynamic antimicrobial activity against *Helicobacter pylori in vitro* [165]. Only 1 log was killed by MB-PDI while 7 logs were killed by the combination of MB-chitosan and endoscopic white light.

Cellulose

Cellulose (Figure 11B) is a natural biopolymer and one of the most naturally abundant biomaterials on the planet. It possesses a high molecular weight, and its structural motif consists of a number of (β-1,4-linked anhydro-D-glucose) polymer chains. It is considered to be an outstanding material for developing promising new biomaterials from renewable plant resources [166]. Cellulose has a very regular structure composed of crystalline units or nanodomains. On acidic hydrolysis bulk cellulose produces highly crystalline rod-shaped cellulose nanocrystals (100–400 nm in length) with high mechanical strength and is easily able to be chemically modified due to the hydroxyl groups [167–169].

Cellulose nanocrystals (CNC) are very attractive starting materials to produce high melting point composites, thermal extrusions and heat-resistant materials [170]. CNC can be used as scaffolds for fabricating nanomaterials because of their unique chemical and physical characteristics that allows formation of rigid molecular rods with well-controlled dimensions, enantiopurity and the presence of primary hydroxyl groups at the C6 position for chemical modification. CNC provided a novel starting material for the preparation of a unique photobactericidal material [171,172]. CNC-Por(1) is a photobactericidal material formed by the covalent attachment of an alkyne-containing porphyrin PS (Figure 10G) to the surface of azide-modified cellulose nanocrystals using the Cu(I)-catalyzed Huisgen-Meldal-Sharpless 1,3-dipolar cycloaddition reaction (better known as Click Chemistry) [173]. Studies showed that CNC-Por(1) could mediate PDI of both methicillin-susceptible *S. aureus* (MSSA) and *M. smegmatis* (as a substitute for *M. tuberculosis*), however, the bactericidal activity was very low in case of *E. coli* [173,174]. Another study by the same group tested CNC-Por(1) against *Acinetobacter baumannii*, multiple-drug resistant *A. baumannii* (MDRAB), MRSA and *P. aeruginosa*. They concluded that (regardless of the material being an insoluble suspension) CNC-Por(1) had a broad spectrum antimicrobial activity. Upon illumination with visible light (400–700 nm; 118 J/cm^2) excellent antimicrobial activity against *A. baumannii*, MSSA and MRSA was observed, with a 5–6 log units reduction in CFUs [174]. However, *P. aeruginosa* was only moderately photo-inactivated by CNC-Por(1) with 2–3 log CFU reduction [174].

Gold & silver nanoparticles

The biocompatibility of Au nanoparticles has encouraged their extensive utilization in many different organisms [175,176]. Gold nanoparticles (Au) are generally considered to be biologically inert, but they absorb light that can produce a significant photothermal effect. Gold nanoparticles can be used as drug delivery platforms, similar to other inorganic nanoparticles or as surface plasmon-enhanced agents taking account of the nonlinear optical fields that come into effect at very close distances to metal nanoparticles. Both these types of application have been employed in photodynamic therapy, showed in Figure 12. [124]. Au-based nanomaterials such as Au nanospheres, Au nanocages and Au nanorods with characteristic near-infrared absorption can produce photothermal destruction of bacteria. Au nanorods conjugated with PS can kill MRSA by a combination of PACT and photothermal effect [177,178]. *S. aureus* can be killed using laser activation of Au nanoparticles conjugated with specific antibodies [179] via a photothermal effect killing pathogens [180–182]. Gold nanoparticles have been shown to have intrinsic antibacterial activity against MRS, VRE, *E. coli, P. aeruginosa* [183–185].

Kuo *et al.* conjugated the hydrophilic PS, toluidine blue O (TBO; Figure 10H), to the surface of Au nanorods for PACT and found that this conjugated Au-PAA-TBO nanorods acted as dual-function agents producing both PDI and hyperthermia against MRSA, acting simultaneously as photodynamic and photothermal agents to kill MRSA [177]. The concanavalin A-induced clustering of dextran-coated Au nanoparticles suggested that Dex-Au-NP could sense the presence of complex carbohydrates on bacterial cells suspensions, and could provide a nanoparticle-based antimicrobial antibiotic susceptibility assay. This would take advantage of differential changes in the surface plasmon resonance band of Dex-

Au-NP. This method would be much quicker in comparison to traditional culture methods [186].

Combining antibiotics with Au nanoparticles can increase the efficacy of the antibacterial activity [187]. Au-NP coated with vancomycin increased antimicrobial activity against vancomycin resistant *Enterococci* (VRE) [185–188]. Coating Cefaclor (a second-generation β-lactam antibiotic) [189] and ampicillin(C-AuNp-Amp) [190] onto Au nanoparticles increased antimicrobial activity against Gram-positive (*S. aureus*) and Gram-negative bacteria (*E. coli*). Au nanoparticles also enhanced methylene blue-induced PDI against *C. albicans* biofilms [191]. Au nanoparticles have also been shown to have anti-HIV activity and can inhibit several strains of influenza virus by blocking viral attachment to the cell surface [192,193].

Silver has long been known to be antimicrobial due to the high affinity of Ag toward the sulfur and phosphorus atoms in biomolecules [194]. Ag nanoparticles can react with sulfur containing amino acids in the cell membrane that will affect cell viability, and can also react with sulfur containing moieties inhibiting enzyme function involved in DNA replication [195–197] causing cell death [198]. Ag nanoparticles have a dose [199–201], particle size [198,202,203], total surface area [204–206] and shape dependent effect on both Gram-positive and Gram-negative bacteria [207]. The antimicrobial effect of silver is dependent on superficial contact [208]. The higher antimicrobial effect of Ag nanoparticles at lower concentrations than Au or zinc nanoparticles against *S. mutans* suggested that clinical effects might be achieved with reduced toxicity [209]. Another study investigated the antimicrobial activity of Ag, TiO_2 and silica nanoparticles against *S. mutans* as compared with chlorhexidine, a routine disinfectant and found that Ag NPs performed better than chlorhexidine [210].

Ag nanoparticles also have an effect on the cell morphology of *E. coli* and *S. aureus* [211,212]. The biocidal property is mainly due to Ag ions released from Ag nanoparticles and to a coating of silver oxide on these nanoparticles [202]. The composite Ag nanoparticles formed with polymers could increase the antimicrobial effect of Ag nanoparticles alone [213–215]. The nano-Ag had antibacterial action against *E. coli* [216] and involved alterations of the expression of a number of envelope proteins (OmpA, OmpC, OmpF, OppA and MetQ) and heat shock proteins (IbpA and IbpB) [217,218]. Moreover nano-Ag was more efficient than Ag salts alone as an antimicrobial agent against *Vibrio cholerae* [201].

Antimicrobial activity was studied using size-controlled Ag colloid nanoparticles generated by a one-step modified Tollens process against drug resistant pathogens [203]. It was found that nanoparticles with a size less than 25 nm showed minimum inhibitory concentration of 6.75–54 μg/ml and >25 nm sized nanoparticles showed minimum inhibitory concentration in the range of 1.69–13.5 μg/ml against highly MDR bacteria such as MRSA, methicillin-resistant coagulase-negative *Staphylococci* (*S. epidermidis*), vancomycin-resistant *E. faecium* and ESBL-positive *K. pneumoniae*. Ag nanoparticles had the highest activity against MRSA followed by MRSE and *Streptococcus pyogenes* and moderate antimicrobial activity against *Salmonella typhi* and *K. pneumoniae* [219].

Brown *et al.* suggested that when ampicillin was bound to the surfaces of Ag NP and AuNP, their intrinsic antibacterial activity could be significantly increased. Both AuNP and AgNP when functionalized with ampicillin became potent antibacterial agents and could overcome antibiotic resistance mechanisms of MDR bacteria, and could kill pathogenic *E. coli, V. cholerae, Enterobacter aerogenes*, MRSA and *P. aeruginosa* [220].

Ag nanoparticles inhibited HIV-1, Influenza virus, Herpes Simplex virus, Respiratory syncytial virus and Monkey pox virus by blocking the viral attachment to the cell surface [193,221–224]. Ag-nanoparticles also have fungicidal and fungistatic effects on the dermatophytes *Trichophyton mentagrophytes* and *Candida* species by disrupting the cell membrane [225–227].

Silica

Silica (SiO_2) is a mineral that is a major component of sand and glass, and has also been used in the synthesis of nanoparticles. Many different functional groups can be added to the surface of silica nanoparticles (SiNPs). These SiNPs serve as a potential carrier for PDT/PDI applications [228]. SiNPs can be prepared with well-controlled particle size, shape, porosity and monodisperse distribution. Moreover, numerous different PS can be encapsulated, SiNPs are not subject to microbial attack, are stable to changes in pH, and there occurs no swelling or change in porosity in biological environments. Due to the permeability of the porous matrix to molecular oxygen, singlet oxygen that is generated inside can come out, so the photodestructive effect can be maintained in encapsulated form [124]. Various preparation methods have been reported such as organically modified silicates (ORMOSIL), hollow silica, mesoporous SiNPs (MSN), the Stöber procedure to generate amorphous SiNPs of a controlled size, the reverse microemulsion (water-in-oil) method, and recently a direct microemulsion (oil-in-water) procedure and the sol-gel method have all been used to prepare nanoparticles for PDT [229–231]. As mentioned above most PS are poorly soluble and easily form nonphotoactive aggregates, so there is a need for effective drug-delivery vehicles [110]. Nanoparticle-based PS have an advantage over free PS molecules, as NP encapsulation makes the dyes more resistant toward photobleaching, and the concentrated but not quenched PS molecules present on the nanoparticle surface enables a higher concentration of locally generated singlet oxygen to cause more damage to the target bacteria [54]. Immobilization of the PS inside or on the surface of the SiNPs can be accomplished by noncovalent encapsulation (most frequently described) and by covalent conjugation (more efficient) [230]. This immobilization or encapsulation will protect the PS from degradation, and the encapsulated form will have superior photostability, higher yield of ROS generation, increased photodynamic efficacy and better aqueous solubility than the free form [124].

Guo *et al.* developed a nanoparticle-based PS, consisting of Rose Bengal (RB)-decorated silica (SiO_2–NH_2–RB) nanoparticles, to inactivate both Gram-positive and Gram-negative bacteria (particularly MRSA and *S. epidermidis*) with high efficiency [54]. Another study described quaternary ammonium (QA)-functionalized SiNP that could release NO when excited with light of the correct wavelength, and which exhibited antimicrobial action against both *S. aureus* and *P. aeruginosa*. Nanoparticles with only NO release capabilities

were more effective against *P. aeruginosa*, while particles with only QA-functionality exhibited greater activity toward *S. aureus* and there was an increased bactericidal efficacy against *S. aureus* by combining NO release and QA-functionality on the same particle but no change in activity was seen against *P. aeruginosa*. Moreover the hybrid NO release/QA-functionalized particles were more effective than mixtures of NO-releasing and QA-functionalized particles separately [232].

Magnetic nanoparticles

MRI is a noninvasive imaging technique that can be used to explore cell trafficking, gene expression and detect cancer. Magnetic nanoparticles (MNPs) have been extensively used as MRI contrast agents and show a unique ability to enhance the MR contrast signal [233]. Moreover, it is possible to use an external magnetic field to control the kinetics and biodistribution of MNPs. Magnetic targeting is an encouraging tool for the site-specific delivery of drugs using a field applied outside the body [234]. Figure 13 shows the structure of MNP with biocompatible coating and PS attached by a linker [124].

These MNP possess a high value of saturation magnetization and superparamagnetism. Additionally, functional MNP can easily be separated from the solvent mixture and purified by applying a magnetic field [235]. In a recent study by Choi *et al.*, multifunctional MNPs were conjugated with PS and with vancomycin using a fabrication method involving surface modification of Fe_3O_4 particles [235]. To allow separation of the captured bacteria from the contaminated sites the MNPs consisted of Fe_3O_4 particles conjugated with a PS, [5,15-bisphenyl-10,20-bis(4-methoxycarbonylphenyl)-porphyrin]-platinum (t-PtCP; Figure 10I), and after PDI there could be complete removal of the PS using a magnet. To deliver the MNPs specifically to the bacterial cell membrane they were also functionalized with vancomycin used here as a targeting molecule, not as an antibiotic. The study concluded that MMPs had good biocompatibility, and when excited with 510 nm light they could target, capture and photoinactivate numerous pathogenic bacteria including MRSA and VRE.

Upconversion nanoparticles

Many of the most powerful PS are optimally excited with UV or short wavelength (blue) visible light but these wavelengths possess inadequate tissue penetration ability [236,237]. Upconversion (UC) is a nonlinear optical process that leads to the emission of light at a shorter wavelength than the excitation wavelength (anti-Stokes type emission) following successive absorption of two or more photons [124,238]. Upconversion can be efficiently excited at low peak power densities, contrary to other nonlinear processes based on multiphoton absorption that require peak power densities of the order of 10^{10} W/cm^2. Highly efficient UC nanocrystals are formed from rare earth metal salts and have controlled properties of solubility, particle size, crystallographic phase, optical properties and shape. Nanocrystals are doped with lanthanide ions in the form of solid-state materials and are considered as most efficient for UC [124]. Recent studies have proposed that UC nanoparticles could be alternatives to conventional agents such as organic fluorophosphors and quantum dots in the field of medical optical imaging [238]. Lim *et al.* [236] used near-infrared-to-visible UC nanoparticles (Figure 14) consisting of sodium yttrium fluoride

($NaYF_4$) co-doped with ytterbium (Yb^{3+}) and erbium (Er^{3+}) ions contained inside a PEI shell that was embedded with the PS zinc phthalocyanine to demonstrate UC-based PDI as a prospective antiviral therapy. When excited with 980 nm light the UCN acted as nanotransducers to produce visible light to excite the PS zinc phthalocyanine (ZnPC;Figure 10J) and to produce $^1O_2$. The UCN were effective in reducing titers of both dengue virus serotype 2 (DENV2) and adenovirus type 5 (Ad5V). The viruses were propagated on C6/36 cells and HeLa cells, respectively, that allowed plaque-forming units to be assayed. When light treated DENV2 virus suspension was inoculated into mice it caused no disease [236].

Conclusion & future perspective

The relatively young field of nanotechnology was only invented in 1959 when US physicist Richard P Feynman gave a speech at an American Physical Society meeting at the California Institute of Technology, entitled “There’s plenty of room at the bottom” [239]. This relatively late beginning can be contrasted with the field of photodynamic therapy that was invented over 110 years ago in 1900 when Oscar Raab [240] discovered that certain microorganisms could be killed by particular combinations of dyes and light. Nevertheless the progress made by these two complimentary (if not outright synergistic) technologies has been nothing short of astonishing. As both PDI [241] and nanomedicine [242] progress steadily toward more approved clinical indications, it seems high time that these fields should ‘get together.’ The very real improvements in photosensitizer solubility, photophysics and photochemistry that may be achieved by a judicious choice of a nanoparticle delivery vehicle, will continue to be investigated for ever more broad indications. What promises to be even more exciting, are those applications where the nanomaterial itself takes part in the optics, physics and chemistry of the photodynamic process. Titania photocatalysis with its almost infinite photostability, has the promise to allow the manufacture of a range of self-sterilizing surfaces and tools for biomedical applications. However self-sterilizing surfaces are still so new that their eventual utility and optimal design features are still uncertain. The carbon nanomaterials (fullerenes, nanotubes and graphene) are being discovered to be photoactive in their own right, exhibiting intriguing photoinduced-electron transfer properties. The plasmonic properties of gold and silver nanoparticles again give intriguing hints of greatly potentiated photochemistry occurring under the influence of these locally enhanced electromagnetic fields. Finally the use of rare earth upconversion nanoparticles gives the promise of PDI no longer being limited by the penetration of light in tissue, as inexpensive continuous wave lasers can now produce the required short wavelength light to activate powerful photosensitizers. The following fields of clinical medicine are most likely to benefit from antimicrobial photodynamic nanomedicine, dermatology, dentistry, gynecology, urology, otolaryngology, ophthalmology and others. Altogether, the future looks bright for the long and happy marriage of antimicrobial photodynamic inactivation and nanomedicine.

Acknowledgments

This includes employment, consultancies, honoraria, stock ownership or options, expert testimony, grants or patents received or pending, or royalties.

References

Papers of special note have been highlighted as:

• of interest; •• of considerable interest

1. Guyer B, Freedman MA, Strobino DM, Sondik EJ. Annual summary of vital statistics: trends in the health of Americans during the 20th century. Pediatrics. 2000; 106(6):1307–1317. [PubMed: 11099582]
2. Fauci AS, Morens DM. The perpetual challenge of infectious diseases. N. Engl. J. Med. 2012; 366(5):454–461. [PubMed: 22296079]
3. Youngblood WJ, Gryko DT, Lammi RK, Bocian DF, Holten D, Lindsey JS. Glaser-mediated synthesis and photophysical characterization of diphenylbutadiyne-linked porphyrin dyads. J. Org. Chem. 2002; 67(7):2111–2117. [PubMed: 11925216]
4. Smith R, Coast J. The true cost of antimicrobial resistance. Br. Med. J. 2013; 346:f1493. [PubMed: 23479660]
5. Kraus CN. Low hanging fruit in infectious disease drug development. Curr. Opin. Microbiol. 2008; 11(5):434–438. [PubMed: 18822387]
6. Munoz-Price LS, Poirel L, Bonomo RA, et al. Clinical epidemiology of the global expansion of *Klebsiella pneumoniae* carbapenemases. Lancet Infect. Dis. 2013; 13(9):785–796. [PubMed: 23969216]
7. Yoneyama H, Katsumata R. Antibiotic resistance in bacteria and its future for novel antibiotic development. Biosci. Biotechnol. Biochem. 2006; 70(5):1060–1075. [PubMed: 16717405]
8. Hamblin MR, Hasan T. Photodynamic therapy: a new antimicrobial approach to infectious disease? Photochem. Photobiol. Sci. 2004; 3(5):436–450. [PubMed: 15122361]
9. Maisch T. Anti-microbial photodynamic therapy: useful in the future? Lasers Med. Sci. 2007; 22(2): 83–91. [PubMed: 17120167]
10. Maisch T, Hackbarth S, Regensburger J, et al. Photodynamic inactivation of multi-resistant bacteria (PIB) – a new approach to treat superficial infections in the 21st century. J. Dtsch Dermatol. Ges. 2011; 9(5):360–366. [PubMed: 21114627]
11. Bush K, Courvalin P, Dantas G, et al. Tackling antibiotic resistance. Nat. Rev. Microbiol. 2011; 9(12):894–896. [PubMed: 22048738] •• Influential review highlighting the growing danger of microbial drug resistance.
12. Almeida RD, Manadas BJ, Carvalho AP, Duarte CB. Intracellular signaling mechanisms in photodynamic therapy. Biochim. Biophys. Acta. 2004; 1704(2):59–86. [PubMed: 15363861]
13. Johnson GA, Ellis EA, Kim H, Muthukrishnan N, Snavely T, Pellois JP. Photoinduced membrane damage of *E. coli* and *S. aureus* by the photosensitizer-antimicrobial peptide conjugate eosin-(KLAKLAK)2. PLoS ONE. 2014; 9(3):e91220. [PubMed: 24608860]
14. Pereira MA, Faustino MA, Tome JP, et al. Influence of external bacterial structures on the efficiency of photodynamic inactivation by a cationic porphyrin. Photochem. Photobiol. Sci. 2014; 13(4):680–690. [PubMed: 24549049]
15. Malik Z, Hanania J, Nitzan Y. Bactericidal effects of photoactivated porphyrins – an alternative approach to antimicrobial drugs. J. Photochem. Photobiol. B. 1990; 5(3–4):281–293. [PubMed: 2115912]
16. Minnock A, Vernon DI, Schofield J, Griffiths J, Parish JH, Brown ST. Photoinactivation of bacteria. Use of a cationic water-soluble zinc phthalocyanine to photoinactivate both gram-negative and gram-positive bacteria. J. Photochem. Photobiol. B. 1996; 32(3):159–164. [PubMed: 8622179] • Paper highlighting the importance of cationic charges in efficient photosensitizers to kill Gram-negative bacteria.
17. Malik Z, Ladan H, Nitzan Y. Photodynamic inactivation of Gram-negative bacteria: problems and possible solutions. J. Photochem. Photobiol. B. 1992; 14(3):262–266. [PubMed: 1432395] •• One of the first papers highlighting the difficulty faced by attempts to use photosensitizers normally used to kill cancer cells, to kill Gram-negative bacteria.

18. Lambert PA. Cellular impermeability and uptake of biocides and antibiotics in Gram-positive bacteria and mycobacteria. J. Appl. Microbiol. 2002; 92(Suppl.):S46–S54.
19. Minnock A, Vernon DI, Schofield J, Griffiths J, Parish JH, Brown SB. Mechanism of uptake of a cationic water-soluble pyridinium zinc phthalocyanine across the outer membrane of *Escherichia coli*. Antimicrob. Agents Chemother. 2000; 44(3):522–527. [PubMed: 10681312]
20. Nitzan Y, Gutterman M, Malik Z, Ehrenberg B. Inactivation of gram-negative bacteria by photosensitized porphyrins. Photochem. Photobiol. 1992; 55(1):89–96. [PubMed: 1534909]
21. Valduga G, Bertoloni G, Reddi E, Jori G. Effect of extracellularly generated singlet oxygen on Gram-positive and Gram-negative bacteria. J. Photochem. Photobiol. B. 1993; 21(1):81–86. [PubMed: 8289115]
22. Nishiyama N, Nakagishi Y, Morimoto Y, et al. Enhanced photodynamic cancer treatment by supramolecular nanocarriers charged with dendrimer phthalocyanine. J. Control. Release. 2009; 133(3):245–251. [PubMed: 19000725]
23. Mills A, Le Hunte S. An overview of semiconductor photocatalysis. J. Photochem. Photobiol. A Chem. 1997; 108(1):1–35.
24. Hashimoto K. TiO_2 photocatalysis: a historical overview and future prospects. Jpn. J. Appl. Phys. 2005; 44(12):8269–8285. (Pt 8261).
25. Wong CC, Chu W. The hydrogen peroxide-assisted photocatalytic degradation of alachlor in TiO_2 suspensions. Environ. Sci. Technol. 2003; 37(10):2310–2316. [PubMed: 12785542]
26. Spesia MB, Milanesio ME, Durantini EN. Synthesis, properties and photodynamic inactivation of *Escherichia coli* by novel cationic fullerene C60 derivatives. Eur. J. Med. Chem. 2008; 43(4):853–861. [PubMed: 17706838]
27. Jori G, Brown SB. Photosensitized inactivation of microorganisms. Photochem. Photobiol. Sci. 2004; 3(5):403–405. [PubMed: 15122355]
28. Soncin M, Fabris C, Busetti A, et al. Approaches to selectivity in the Zn(II)-phthalocyanine-photosensitized inactivation of wild-type and antibiotic-resistant *Staphylococcus aureus*. Photochem. Photobiol. Sci. 2002; 1(10):815–819. [PubMed: 12656484]
29. Lauro FM, Pretto P, Covolo L, Jori G, Bertoloni G. Photoinactivation of bacterial strains involved in periodontal diseases sensitized by porphycene-polylysine conjugates. Photochem. Photobiol. Sci. 2002; 1(7):468–470. [PubMed: 12659156]
30. Huang L, Terakawa M, Zhiyentayev T, et al. Innovative cationic fullerenes as broad-spectrum light-activated antimicrobials. Nanomedicine. 2010; 6(3):442–452. [PubMed: 19914400]
31. Perni S, Prokopovich P, Pratten J, Parkin IP, Wilson M. Nanoparticles: their potential use in antibacterial photodynamic therapy. Photochem. Photobiol. Sci. 2011; 10(5):712–720. [PubMed: 21380441]
32. Felgentrager A, Maisch T, Spath A, Schroder JA, Baumler W. Singlet oxygen generation in porphyrin-doped polymeric surface coating enables antimicrobial effects on Staphylococcus aureus. Phys. Chem. Chem. Phys. 2014; 16(38):20598–20607. [PubMed: 25155698]
33. Zerdin K, Scully AD. Inactivation of food-borne spoilage and pathogenic micro-organisms on the surface of a photoactive polymer. Photochem. Photobiol. 2010; 86(5):1109–1117. [PubMed: 20670362]
34. Bezman SA, Burtis PA, Izod TP, Thayer MA. Photodynamic inactivation of *E. coli* by rose bengal immobilized on polystyrene beads. Photochem. Photobiol. 1978; 28(3):325–329. [PubMed: 360250]
35. Kendall CA, Morton CA. Photodynamic therapy for the treatment of skin disease. Technol. Cancer Res. Treat. 2003; 2(4):283–288. [PubMed: 12892510]
36. Moan J, Peng Q, Sorensen R, Iani V, Nesland JM. The biophysical foundations of photodynamic therapy. Endoscopy. 1998; 30(4):387–391. [PubMed: 9689514]
37. Paszko E, Ehrhardt C, Senge MO, Kelleher DP, Reynolds JV. Nanodrug applications in photodynamic therapy. Photodiagnosis Photodyn. Ther. 2011; 8(1):14–29. [PubMed: 21333931]
38. Derycke AS, De Witte PA. Liposomes for photodynamic therapy. Adv. Drug Deliv. Rev. 2004; 56(1):17–30. [PubMed: 14706443]

39. Zhang GD, Harada A, Nishiyama N, et al. Polyion complex micelles entrapping cationic dendrimer porphyrin: effective photosensitizer for photodynamic therapy of cancer. J. Control. Release. 2003; 93(2):141–150. [PubMed: 14636720]
40. Van Nostrum CF. Polymeric micelles to deliver photosensitizers for photodynamic therapy. Adv. Drug Deliv. Rev. 2004; 56(1):9–16. [PubMed: 14706442]
41. Li B, Moriyama EH, Li F, Jarvi MT, Allen C, Wilson BC. Diblock copolymer micelles deliver hydrophobic protoporphyrin IX for photodynamic therapy. Photochem. Photobiol. 2007; 83(6): 1505–1512. [PubMed: 18028227]
42. Nishiyama N, Morimoto Y, Jang WD, Kataoka K. Design and development of dendrimer photosensitizer-incorporated polymeric micelles for enhanced photodynamic therapy. Adv. Drug Deliv. Rev. 2009; 61(4):327–338. [PubMed: 19385091]
43. Narsireddy A, Vijayashree K, Irudayaraj J, Manorama SV, Rao NM. Targeted *in vivo* photodynamic therapy with epidermal growth factor receptor-specific peptide linked nanoparticles. Int. J. Pharm. 2014; 471(1–2):421–429. [PubMed: 24939618]
44. Yang Y, Hu Y, Du H, Wang H. Intracellular gold nanoparticle aggregation and their potential applications in photodynamic therapy. Chem. Commun. (Camb.). 2014; 50(55):7287–7290. [PubMed: 24871860]
45. Ricci-Junior E, Marchetti JM. Preparation, characterization, photocytotoxicity assay of PLGA nanoparticles containing zinc (II) phthalocyanine for photodynamic therapy use. J. Microencapsul. 2006; 23(5):523–538. [PubMed: 16980274]
46. Roy I, Ohulchanskyy TY, Pudavar HE, et al. Ceramic-based nanoparticles entrapping water-insoluble photosensitizing anticancer drugs: a novel drug-carrier system for photodynamic therapy. J. Am. Chem. Soc. 2003; 125(26):7860–7865. [PubMed: 12823004]
47. Wang L, Shi J, Liu R, et al. Photodynamic effect of functionalized single-walled carbon nanotubes: a potential sensitizer for photodynamic therapy. Nanoscale. 2014; 6(9):4642–4651. [PubMed: 24647856]
48. Xing Y, Dai L. Nanodiamonds for nanomedicine. Nanomedicine (Lond.). 2009; 4(2):207–218. [PubMed: 19193186]
49. Zhang XQ, Chen M, Lam R, Xu X, Osawa E, Ho D. Polymer-functionalized nanodiamond platforms as vehicles for gene delivery. ACS Nano. 2009; 3(9):2609–2616. [PubMed: 19719152]
50. Griffiths G, Nystrom B, Sable SB, Khuller GK. Nanobead-based interventions for the treatment and prevention of tuberculosis. Nat. Rev. Microbiol. 2010; 8(11):827–834. [PubMed: 20938454]
51. Kateb B, Chiu K, Black KL, et al. Nanoplatforms for constructing new approaches to cancer treatment, imaging, and drug delivery: what should be the policy? Neuroimage. 2011; 54(Suppl. 1):S106–S124. [PubMed: 20149882]
52. Casas A, Battah S, Di Venosa G, et al. Sustained and efficient porphyrin generation *in vivo* using dendrimer conjugates of 5-ALA for photodynamic therapy. J. Control. Release. 2009; 135(2):136–143. [PubMed: 19168101]
53. Alarcon E, Edwards AM, Aspee A, Borsarelli CD, Lissi EA. Photophysics and photochemistry of rose bengal bound to human serum albumin. Photochem. Photobiol. Sci. 2009; 8(7):933–943. [PubMed: 19582268]
54. Guo Y, Rogelj S, Zhang P. Rose Bengal-decorated silica nanoparticles as photosensitizers for inactivation of Gram-positive bacteria. Nanotechnology. 2010; 21(6):065102. [PubMed: 20061596]
55. Tang W, Xu H, Kopelman R, Philbert MA. Photodynamic characterization and *in vitro* application of methylene blue-containing nanoparticle platforms. Photochem. Photobiol. 2005; 81(2):242–249. [PubMed: 15595888]
56. Khdair A, Gerard B, Handa H, Mao G, Shekhar MP, Panyam J. Surfactant-polymer nanoparticles enhance the effectiveness of anticancer photodynamic therapy. Mol. Pharm. 2008; 5(5):795–807. [PubMed: 18646775]
57. Suppan, P. Chemistry and Light. Vol. 295. London, UK: Royal Society of Chemistry; 1994.
58. Fujishima A, Honda K. Electrochemical photolysis of water at a semiconductor electrode. Nature. 1972; 238(5358):37–38. [PubMed: 12635268]

59. Herrmann JM. Heterogeneous photocatalysis: fundamentals and applications to the removal of various types of aqueous pollutants. Catal. Today. 1999; 53(1):115–129.
60. Kashyout AB, Soliman M, El-Haleem DA. Disinfection of bacterial suspensions by photocatalytic oxidation using TiO_2 nanoparticles under ultraviolet illumination. Alexandria Eng. 2006; 45(3): 367–371.
61. Cheng CL, Sun DS, Chu WC, et al. The effects of the bacterial interaction with visible-light responsive titania photocatalyst on the bactericidal performance. J. Biomed. Sci. 2009; 16:7. [PubMed: 19272171]
62. Tatsuma T, Takeda S, Saitoh S, Ohko Y, Fujishima A. Bactericidal effect of an energy storage TiO_2–WO_3 photocatalyst in dark. Electrochem. Commun. 2003; 5(9):793–796.
63. Vohra A, Goswami DY, Deshpande DA, Block SS. Enhanced photocatalytic disinfection of indoor air. Appl Catalysis B Environ. 2006; 64(1–2):57–65.
64. Sapkota A, Dutta J. Zinc oxide nanorod mediated visible light photoinactivation of model microbes in water. Nanotechnology. 2011; 22(21):215703. [PubMed: 21451231]
65. Rodriguez J. Solar water disinfection studies with supported TiO_2 and polymer-supported RII) sensitizer in a compound parabolic collector. J. Sol. Energy Eng. Trans ASME. 2007; 132(1): 0110011–0110015.
66. Ditta IB, Steele A, Liptrot C, et al. Photocatalytic antimicrobial activity of thin surface films of $TiO_{(2)}$, CuO and $TiO_{(2)}$/CuO dual layers on *Escherichia coli* and bacteriophage T4. Appl. Microbiol. Biotechnol. 2008; 79(1):127–133. [PubMed: 18317747]
67. Sato T, Koizumi Y, Taya M. Photocatalytic deactivation of airborne microbial cells on TiO_2-loaded plate. Biochem. Eng. J. 2003; 14(2):149–152.
68. Kuhn KP, Chaberny IF, Massholder K, et al. Disinfection of surfaces by photocatalytic oxidation with titanium dioxide and UVA light. Chemosphere. 2003; 53(1):71–77. [PubMed: 12892668]
69. Luo L, Miao L, Tanemura S, Tanemura M. Photocatalytic sterilization of TiO_2 films coated on Al fiber. Mater. Sci. Eng. B. 2008; 148(1–3):183–186.
70. Yao Y, Ohko Y, Sekiguchi Y, Fujishima A, Kubota Y. Self-sterilization using silicone catheters coated with Ag and TiO_2 nanocomposite thin film. J. Biomed. Mater. Res. B Appl. Biomater. 2008; 85(2):453–460. [PubMed: 18098205]
71. Block SS, Seng VP, Goswami DW. Chemically enhanced sunlight for killing bacteria. J. Sol. Energy Eng. 1997; 119(1):85.
72. Goswami T. Photocatalytic system to destroy bioaerosols in air. J. Adv. Oxid. Technol. 1999; 4:185–188.
73. Song S. Fabrication of TiO_2 impregnated stainless steel fiber photocatalyts and evaluation of photocatalytic activity. J. Korean Ind. Eng. Chem. 2008; 19(6):674–679.
74. Cho M, Choi Y, Park H, Kim K, Woo GJ, Park J. Titanium dioxide/UV photocatalytic disinfection in fresh carrots. J. Food Prot. 2007; 70(1):97–101. [PubMed: 17265866]
75. Armon R. Disinfection of *Bacillus* spp. spores in drinking water by TiO_2 photocatalysis as a model for *Bacillus anthracis*. Waterborne Pathog. 2004; 4(2):7–14.
76. Butterfield IM. Water disinfection using an immobilised titanium dioxide film in a photochemical reactor with electric field enhancement. Water Res. 1997; 31(3):675–677.
77. Guimarães JR, Barretto AS. Photocatalytic inactivation of Clostridium perfringens and coliphages in water. Braz. J. Chem. Eng. 2003; 20:403–411.
78. Singh A. Photocatalytic disinfection of water using immobilized titanium dioxide. Poll. Res. 2005; 24(1):29–33.
79. Vidal A, DíAz AI, El Hraiki A, et al. Solar photocatalysis for detoxification and disinfection of contaminated water: pilot plant studies. Catal. Today. 1999; 54(2–3):283–290.
80. Chen WJ, Tsai PJ, Chen YC. Functional Fe_3O_4/TiO_2 core/shell magnetic nanoparticles as photokilling agents for pathogenic bacteria. Small. 2008; 4(4):485–491. [PubMed: 18348230]
81. Oka Y, Kim WC, Yoshida T, et al. Efficacy of titanium dioxide photocatalyst for inhibition of bacterial colonization on percutaneous implants. J. Biomed. Mater. Res. B Appl. Biomater. 2008; 86(2):530–540. [PubMed: 18386839]

82. Chen F, Yang X, Wu Q. Antifungal capability of TiO_2 coated film on moist wood. Build. Environ. 2009; 44(5):1088–1093.
83. Wolfrum EJ, Huang J, Blake DM, et al. Photocatalytic oxidation of bacteria, bacterial and fungal spores, and model biofilm components to carbon dioxide on titanium dioxide-coated surfaces. Environ. Sci. Technol. 2002; 36(15):3412–3419. [PubMed: 12188373]
84. Erkan A. Photocatalytic microbial inactivation over Pd doped SnO_2 and TiO_2 thin films. J. Photoch. Photobiol. A Chem. 2006; 184(3):313–321.
85. Sokmen M, Degerli S, Aslan A. Photocatalytic disinfection of *Giardia intestinalis* and *Acanthamoeba castellani* cysts in water. Exp. Parasitol. 2008; 119(1):44–48. [PubMed: 18255065]
86. Ryu H. Photocatalytic inactivation of *Cryptosporidium parvum* with TiO_2 and low-pressure ultraviolet irradiation. Water. Res. 2008; 42(6–7):1523–1530. [PubMed: 18037465]
87. Guillard C, Bui T-H, Felix C, Moules V, Lina B, Lejeune P. Microbiological disinfection of water and air by photocatalysis. C. R. Chim. 2008; 11(1–2):107–113.
88. Zan L, Fa W, Peng T, Gong ZK. Photocatalysis effect of nanometer TiO_2 and TiO_2-coated ceramic plate on hepatitis B virus. J. Photochem. Photobiol. B. 2007; 86(2):165–169. [PubMed: 17055286]
89. Lin Z. Inactivation efficiency of TiO_2 on H1N1 influenza virus. Gaodeng Xuexiao Huaxue Xuebao Chem. J. Chin. Univ. 2006; 27(4):721–725.
90. Kozlova EA, Safatov AS, Kiselev SA, et al. Inactivation and mineralization of aerosol deposited model pathogenic microorganisms over TiO_2 and Pt/TiO_2 . Environ. Sci. Technol. 2010; 44(13): 5121–5126. [PubMed: 20521809]
91. Watts RJ, Kong S, Orr MP, Miller GC, Henry BE. Photocatalytic inactivation of coliform bacteria and viruses in secondary wastewater effluent. Water Res. 1995; 29(1):95–100.
92. Han W, Zhang B, Cao W, et al. The inactivation effect of photocatalytic titanium apatite filter on SARS virus. Sheng wu hua xue yu sheng wu wu li jin zhan. 2003; 31(11):982–985.
93. Sekiguchi Y, Yao Y, Ohko Y, et al. Self-sterilizing catheters with titanium dioxide photocatalyst thin films for clean intermittent catheterization: basis and study of clinical use. Int. J. Urol. 2007; 14(5):426–430. [PubMed: 17511726]
94. Nakamura H, Tanaka M, Shinohara S, Gotoh M, Karube I. Development of a self-sterilizing lancet coated with a titanium dioxide photocatalytic nano-layer for self-monitoring of blood glucose. Biosens. Bioelectron. 2007; 22(9–10):1920–1925. [PubMed: 16987650]
95. Chawengkijwanich C, Hayata Y. Development of TiO_2 powder-coated food packaging film and its ability to inactivate *Escherichia coli in vitro* and in actual tests. Int. J. Food Microbiol. 2008; 123(3):288–292. [PubMed: 18262298]
96. Suketa N, Sawase T, Kitaura H, et al. An antibacterial surface on dental implants, based on the photocatalytic bactericidal effect. Clin. Implant Dent. Relat. Res. 2005; 7(2):105–111. [PubMed: 15996357] • Useful application of titania photocatalysis to make self-sterilizing dental implants.
97. Lilja M, Forsgren J, Welch K, Astrand M, Engqvist H, Stromme M. Photocatalytic and antimicrobial properties of surgical implant coatings of titanium dioxide deposited though cathodic arc evaporation. Biotechnol. Lett. 2012; 34(12):2299–2305. [PubMed: 22941372]
98. Sharma SK, Chiang LY, Hamblin MR. Photodynamic therapy with fullerenes *in vivo*: reality or a dream? Nanomedicine (Lond.). 2011; 6(10):1813–1825. [PubMed: 22122587]
99. Liu Q, Cui Q, Li XJ, Jin L. The applications of buckminsterfullerene C60 and derivatives in orthopaedic research. Connect. Tissue Res. 2014; 55(2):71–79. [PubMed: 24409811]
100. Gunes S, Neugebauer H, Sariciftci NS. Conjugated polymer-based organic solar cells. Chem. Rev. 2007; 107(4):1324–1338. [PubMed: 17428026]
101. Arias AC, Mackenzie JD, Mcculloch I, Rivnay J, Salleo A. Materials and applications for large area electronics: solution-based approaches. Chem. Rev. 2010; 110(1):3–24. [PubMed: 20070114]
102. Kang H, Cho CH, Cho HH, et al. Controlling number of indene solubilizing groups in multiadduct fullerenes for tuning optoelectronic properties and open-circuit voltage in organic solar cells. ACS Appl. Mater. Interfaces. 2012; 4(1):110–116. [PubMed: 22148504]
103. Mizuno K, Zhiyentayev T, Huang L, et al. Antimicrobial photodynamic therapy with functionalized fullerenes: quantitative structure-activity relationships. J. Nanomed. Nanotechnol. 2011; 2(2):1–9. [PubMed: 21743839]

104. Mroz P, Pawlak A, Satti M, et al. Functionalized fullerenes mediate photodynamic killing of cancer cells: type I versus type II photochemical mechanism. Free Radic. Biol. Med. 2007; 43(5): 711–719. [PubMed: 17664135]

105. Mroz P, Tegos GP, Gali H, Wharton T, Sarna T, Hamblin MR. Photodynamic therapy with fullerenes. Photochem. Photobiol. Sci. 2007; 6(11):1139–1149. [PubMed: 17973044]

106. Tegos GP, Demidova TN, Arcila-Lopez D, et al. Cationic fullerenes are effective and selective antimicrobial photosensitizers. Chem. Biol. 2005; 12(10):1127–1135. [PubMed: 16242655]

107. Lu Z, Dai T, Huang L, et al. Photodynamic therapy with a cationic functionalized fullerene rescues mice from fatal wound infections. Nanomedicine (Lond.). 2010; 5(10):1525–1533. [PubMed: 21143031] •• One of the few papers to use fullerenes to save the life of mice used antimicrobial photodynamic inactivation.

108. Huang L, Wang M, Sharma SK, et al. Decacationic [70]fullerene approach for efficient photokilling of infectious bacteria and cancer cells. ECS Trans. 2013; 45(20)

109. Wang M, Maragani S, Huang L, et al. Synthesis of decacationic [60] fullerene decaiodides giving photoinduced production of superoxide radicals and effective PDT-mediation on antimicrobial photoinactivation. Eur. J. Med. Chem. 2013; 63C:170–184. [PubMed: 23474903]

110. Wang M, Huang L, Sharma SK, et al. Synthesis and photodynamic effect of new highly photostable decacationically armed [60]- and [70]fullerene decaiodide monoadducts to target pathogenic bacteria and cancer cells. J. Med. Chem. 2012; 55(9):4274–4285. [PubMed: 22512669]

111. Manjon F, Santana-Magana M, Garcia-Fresnadillo D, Orellana G. Are silicone-supported [C60]-fullerenes an alternative to Ru(II) polypyridyls for photodynamic solar water disinfection? Photochem. Photobiol. Sci. 2014; 13(2):397–406. [PubMed: 24395285]

112. Aoshima H, Kokubo K, Shirakawa S, Ito M, Yamana S, Oshima T. Antimicrobial activity of fullerenes and their hydroxylated derivatives. Biocontrol. Sci. 2009; 14(2):69–72. [PubMed: 19579658]

113. Iijima S. Helical microtubules of graphitic carbon. Nature. 1991; 354(6348):56–58.

114. Baughman RH, Zakhidov AA, De Heer WA. Carbon nanotubes – the route toward applications. Science. 2002; 297(5582):787–792. [PubMed: 12161643]

115. Chen P, Wu X, Lin J, Tan KL. High H2 uptake by alkali-doped carbon nanotubes under ambient pressure and moderate temperatures. Science. 1999; 285(5424):91–93. [PubMed: 10390369]

116. Hussain CM, Saridara C, Mitra S. Microtrapping characteristics of single and multi-walled carbon nanotubes. J. Chromatogr. A. 2008; 1185(2):161–166. [PubMed: 18282580]

117. Jolles P, Jolles J. What's new in lysozyme research? Always a model system, today as yesterday. Mol. Cell Biochem. 1984; 63(2):165–189. [PubMed: 6387440]

118. Nepal D, Balasubramanian S, Simonian AL, Davis VA. Strong antimicrobial coatings: single-walled carbon nanotubes armored with biopolymers. Nano Lett. 2008; 8(7):1896–1901. [PubMed: 18507479]

119. Banerjee I, Douaisi MP, Mondal D, Kane RS. Light-activated nanotube-porphyrin conjugates as effective antiviral agents. Nanotechnology. 2012; 23(10):105101. [PubMed: 22361811]

120. Oza G, Pandey S, Gupta A, et al. Photocatalysis-assisted water filtration: using TiO_2-coated vertically aligned multi-walled carbon nanotube array for removal of *Escherichia coli* O157:H7. Mater. Sci. Eng. C Mater. Biol. Appl. 2013; 33(7):4392–4400. [PubMed: 23910358]

121. Dinu CZ, Zhu G, Bale SS, et al. Enzyme-based nanoscale composites for use as active decontamination surfaces. Adv. Funct. Mater. 2010; 20(3):392–398.

122. Wang Y, Li Z, Wang J, Li J, Lin Y. Graphene and graphene oxide: biofunctionalization and applications in biotechnology. Trends Biotechnol. 2011; 29(5):205–212. [PubMed: 21397350]

123. Sun X, Liu Z, Welsher K, et al. Nano-graphene oxide for cellular imaging and drug delivery. Nano Res. 2008; 1(3):203–212. [PubMed: 20216934]

124. Huang YY, Sharma SK, Dai T, et al. Can nanotechnology potentiate photodynamic therapy? Nanotech. Rev. 2012; 10(2):111–146. • Interesting critical review examinaing the role of nanotechnology in potentiating photodynamic therapy (PDT) both against cancer and against infections.

125. Rong P, Yang K, Srivastan A, et al. Photosensitizer loaded nano-graphene for multimodality imaging guided tumor photodynamic therapy. Theranostics. 2014; 4(3):229–239. [PubMed: 24505232]

126. Zhou L, Zhou L, Wei S, et al. Combination of chemotherapy and photodynamic therapy using graphene oxide as drug delivery system. J. Photochem. Photobiol. B. 2014; 135:7–16. [PubMed: 24792568]

127. Sahu A, Choi WI, Lee JH, Tae G. Graphene oxide mediated delivery of methylene blue for combined photodynamic and photothermal therapy. Biomaterials. 2013; 34(26):6239–6248. [PubMed: 23706688]

128. Ristic BZ, Milenkovic MM, Dakic IR, et al. Photodynamic antibacterial effect of graphene quantum dots. Biomaterials. 2014; 35(15):4428–4435. [PubMed: 24612819] • Study using graphene quantum dots to mediate PDT killing of bacteria.

129. Sun H, Gao N, Dong K, Ren J, Qu X. Graphene quantum dots-band-AIDS used for wound disinfection. ACS Nano. 2014; 8(6):6202–6210. [PubMed: 24870970]

130. Bangham AD. A correlation between surface charge and coagulant action of phospholipids. Nature. 1961; 192:1197–1198. [PubMed: 13864660]

131. Sadasivam M, Avci P, Gupta GK, et al. Self-assembled liposomal nanoparticles in photodynamic therapy. Eur. J. Nanomed. 2013; 5(3):115–129.

132. Kozlowska D, Foran P, Macmahon P, Shelly MJ, Eustace S, O'Kennedy R. Molecular and magnetic resonance imaging: the value of immunoliposomes. Adv. Drug Deliv. Rev. 2009; 61(15):1402–1411. [PubMed: 19796661]

133. Vemuri S, Rhodes CT. Preparation and characterization of liposomes as therapeutic delivery systems: a review. Pharm. Acta Helv. 1995; 70(2):95–111. [PubMed: 7651973]

134. Samad A, Sultana Y, Aqil M. Liposomal drug delivery systems: an update review. Curr. Drug Deliv. 2007; 4(4):297–305. [PubMed: 17979650]

135. Kim HJ, Jones MN. The delivery of benzyl penicillin to Staphylococcus aureus biofilms by use of liposomes. J. Liposome Res. 2004; 14(3–4):123–139. [PubMed: 15676122]

136. Mugabe C, Azghani AO, Omri A. Liposome-mediated gentamicin delivery: development and activity against resistant strains of *Pseudomonas aeruginosa* isolated from cystic fibrosis patients. J. Antimicrob. Chemother. 2005; 55(2):269–271. [PubMed: 15590716]

137. Pinto-Alphandary H, Andremont A, Couvreur P. Targeted delivery of antibiotics using liposomes and nanoparticles: research and applications. Int. J. Antimicrob. Agents. 2000; 13(3):155–168. [PubMed: 10724019]

138. Ferro S, Ricchelli F, Mancini G, Tognon G, Jori G. Inactivation of methicillin-resistant *Staphylococcus aureus* (MRSA) by liposome-delivered photosensitising agents. J. Photochem. Photobiol. B. 2006; 83(2):98–104. [PubMed: 16446097]

139. Ferro S, Ricchelli F, Monti D, Mancini G, Jori G. Efficient photoinactivation of methicillin-resistant *Staphylococcus aureus* by a novel porphyrin incorporated into a poly-cationic liposome. Int. J. Biochem. Cell. Biol. 2007; 39(5):1026–1034. [PubMed: 17387034]

140. Bombelli C, Bordi F, Ferro S, et al. New cationic liposomes as vehicles of m-tetrahydroxyphenylchlorin in photodynamic therapy of infectious diseases. Mol. Pharm. 2008; 5(4):672–679. [PubMed: 18507469]

141. Haldar J, Kondaiah P, Bhattacharya S. Synthesis and antibacterial properties of novel hydrolyzable cationic amphiphiles. Incorporation of multiple head groups leads to impressive antibacterial activity. J. Med. Chem. 2005; 48(11):3823–3831. [PubMed: 15916434]

142. Yang YT, Chien HF, Chang PH, et al. Photodynamic inactivation of chlorin e6-loaded CTAB-liposomes against *Candida albicans*. Lasers Surg. Med. 2013; 45(3):175–185. [PubMed: 23508377]

143. Yang K, Gitter B, Ruger R, et al. Antimicrobial peptide-modified liposomes for bacteria targeted delivery of temoporfin in photodynamic antimicrobial chemotherapy. Photochem. Photobiol. Sci. 2011; 10(10):1593–1601. [PubMed: 21773628]

144. Brancaleon L, Moseley H. Laser and non-laser light sources for photodynamic therapy. Lasers Med. Sci. 2002; 17(3):173–186. [PubMed: 12181632]

145. Phillip MJ, Maximuke PP. Chemiluminescence and hematoporphyrin derivative: a novel therapy for mammary adenocarcinomas in mice. Oncology. 1989; 46(4):266–272. [PubMed: 2662091]

146. Carpenter S, Fehr MJ, Kraus GA, Petrich JW. Chemiluminescent activation of the antiviral activity of hypericin: a molecular flashlight. Proc. Natl Acad. Sci. USA. 1994; 91(25):12273–12277. [PubMed: 7991618]

147. Nakonechny F, Firer MA, Nitzan Y, Nisnevitch M. Intracellular antimicrobial photodynamic therapy: a novel technique for efficient eradication of pathogenic bacteria. Photochem. Photobiol. 2010; 86(6):1350–1355. [PubMed: 20880227]

148. Langer R. Biomaterials in drug delivery and tissue engineering: one laboratory's experience. Acc. Chem. Res. 2000; 33(2):94–101. [PubMed: 10673317]

149. Zhang Z, Ortiz O, Goyal R, Kohn J. Biodegradable polymers. Princip. Tissue Eng. 2014; (23): 441–490.

150. Coenye T, Honraet K, Rigole P, Nadal Jimenez P, Nelis HJ. *In vitro* inhibition of *Streptococcus mutans* biofilm formation on hydroxyapatite by subinhibitory concentrations of anthraquinones. Antimicrob. Agents Chemother. 2007; 51(4):1541–1544. [PubMed: 17220400]

151. Nafee N, Youssef A, El-Gowelli H, Asem H, Kandil S. Antibiotic-free nanotherapeutics: hypericin nanoparticles thereof for improved *in vitro* and *in vivo* antimicrobial photodynamic therapy and wound healing. Int. J. Pharm. 2013; 454(1):249–258. [PubMed: 23834835]

152. Pagonis TC, Chen J, Fontana CR, et al. Nanoparticle-based endodontic antimicrobial photodynamic therapy. J. Endod. 2010; 36(2):322–328. [PubMed: 20113801] • Points out an interesting clinical application of nanotechnology-enabled antimicrobial PDT in endodontic therapy.

153. Harris F, Chatfield LK, Phoenix DA. Phenothiazinium based photosensitisers – photodynamic agents with a multiplicity of cellular targets and clinical applications. Curr. Drug Targets. 2005; 6(5):615–627. [PubMed: 16026282]

154. Helander IM, Nurmiaho-Lassila EL, Ahvenainen R, Rhoades J, Roller S. Chitosan disrupts the barrier properties of the outer membrane of gram-negative bacteria. Int. J. Food Microbiol. 2001; 71(2–3):235–244. [PubMed: 11789941]

155. Muzzarelli R, Tarsi R, Filippini O, Giovanetti E, Biagini G, Varaldo PE. Antimicrobial properties of N-carboxybutyl chitosan. Antimicrob. Agents Chemother. 1990; 34(10):2019–2023. [PubMed: 2291669]

156. Ueno H, Mori T, Fujinaga T. Topical formulations and wound healing applications of chitosan. Adv. Drug Deliv. Rev. 2001; 52(2):105–115. [PubMed: 11718934]

157. Ueno H, Yamada H, Tanaka I, et al. Accelerating effects of chitosan for healing at early phase of experimental open wound in dogs. Biomaterials. 1999; 20(15):1407–1414. [PubMed: 10454012]

158. Wang XH, Li DP, Wang WJ, et al. Crosslinked collagen/chitosan matrix for artificial livers. Biomaterials. 2003; 24(19):3213–3220. [PubMed: 12763448]

159. Shimono N, Takatori T, Ueda M, Mori M, Higashi Y, Nakamura Y. Chitosan dispersed system for colon-specific drug delivery. Int. J. Pharm. 2002; 245(1–2):45–54. [PubMed: 12270241]

160. Raafat D, Von Bargen K, Haas A, Sahl HG. Insights into the mode of action of chitosan as an antibacterial compound. Appl. Environ. Microbiol. 2008; 74(12):3764–3773. [PubMed: 18456858]

161. Calvo P, Remuñán-López C, Vila-Jato JL, Alonso MJ. Novel hydrophilic chitosan-polyethylene oxide nanoparticles as protein carriers. J. Appl. Poly Sci. 1997; 63(1):125–132.

162. Shrestha A, Kishen A. Antibacterial efficacy of photosensitizer functionalized biopolymeric nanoparticles in the presence of tissue inhibitors in root canal. J. Endod. 2014; 40(4):566–570. [PubMed: 24666913]

163. Shrestha A, Kishen A. Polycationic chitosan-conjugated photosensitizer for antibacterial photodynamic therapy. Photochem. Photobiol. 2012; 88(3):577–583. [PubMed: 22044238]

164. Chen CP, Chen CT, Tsai T. Chitosan nanoparticles for antimicrobial photodynamic inactivation: characterization and *in vitro* investigation. Photochem. Photobiol. 2012; 88(3):570–576. [PubMed: 22283820]

165. Choi S, Lee H, Chae H. Synergistic *in vitro* photodynamic antimicrobial activity of methylene blue and chitosan against. Helicobacter pylori 26695. Photodiagnosis Photodyn. Ther. 2014; 11(4):526–532. [PubMed: 25174558]
166. Habibi Y, Lucia LA, Rojas OJ. Cellulose nanocrystals: chemistry, self-assembly, and applications. Chem. Rev. 2010; 110(6):3479–3500. [PubMed: 20201500]
167. Araki J, Wada M, Kuga S, Okano T. Flow properties of microcrystalline cellulose suspension prepared by acid treatment of native cellulose. Colloids Surf. A Physicochem. Eng. Asp. 1998; 142(1):75–82.
168. Araki J, Wada M, Kuga S, Okano T. Influence of surface charge on viscosity behavior of cellulose microcrystal suspension. J. Wood. Sci. 1999; 45(3):258–261.
169. Beck-Candanedo S, Roman M, Gray DG. Effect of reaction conditions on the properties and behavior of wood cellulose nanocrystal suspensions. Biomacromolecules. 2005; 6(2):1048–1054. [PubMed: 15762677]
170. Filpponen EI. The synthetic strategies for unique properties in cellulose nanocrystal materials. http://repository.lib.ncsu.edu/ir/bitstream.
171. Rånby BG. Fibrous macromolecular systems. Cellulose and muscle. The colloidal properties of cellulose micelles. Discuss Faraday Soc. 1951; 11:158–164.
172. Filpponen I, Argyropoulos DS. Regular linking of cellulose nanocrystals via click chemistry: synthesis and formation of cellulose nanoplatelet gels. Biomacromolecules. 2010; 11(4):1060–1066. [PubMed: 20235575]
173. Feese E, Sadeghifar H, Gracz HS, Argyropoulos DS, Ghiladi RA. Photobactericidal porphyrin-cellulose nanocrystals: synthesis, characterization, and antimicrobial properties. Biomacromolecules. 2011; 12(10):3528–3539. [PubMed: 21838250]
174. Carpenter BL, Feese E, Sadeghifar H, Argyropoulos DS, Ghiladi RA. Porphyrin-cellulose nanocrystals: a photobactericidal material that exhibits broad spectrum antimicrobial activity. Photochem. Photobiol. 2012; 88(3):527–536. [PubMed: 22360680]
175. Bhattacharya R, Mukherjee P. Biological properties of"naked" metal nanoparticles. Adv. Drug Deliv. Rev. 2008; 60(11):1289–1306. [PubMed: 18501989]
176. Daniel MC, Astruc D. Gold nanoparticles: assembly, supramolecular chemistry, quantum-size-related properties, and applications toward biology, catalysis, and nanotechnology. Chem. Rev. 2004; 104(1):293–346. [PubMed: 14719978]
177. Kuo WS, Chang CN, Chang YT, Yeh CS. Antimicrobial gold nanorods with dual-modality photodynamic inactivation and hyperthermia. Chem. Commun. (Camb.). 2009; (32):4853–4855. [PubMed: 19652803]
178. Pissuwan D, Cortie CH, Valenzuela SM, Cortie MB. Functionalised gold nanoparticles for controlling pathogenic bacteria. Trends Biotechnol. 2010; 28(4):207–213. [PubMed: 20071044]
179. Zharov VP, Mercer KE, Galitovskaya EN, Smeltzer MS. Photothermal nanotherapeutics and nanodiagnostics for selective killing of bacteria targeted with gold nanoparticles. Biophys. J. 2006; 90(2):619–627. [PubMed: 16239330]
180. Norman RS, Stone JW, Gole A, Murphy CJ, Sabo-Attwood TL. Targeted photothermal lysis of the pathogenic bacteria *Pseudomonas aeruginosa* with gold nanorods. Nano Lett. 2008; 8(1): 302–306. [PubMed: 18062714]
181. Simon-Deckers A, Brun E, Gouget B, Carrière M, Sicard-Roselli C. Impact of gold nanoparticles combined to x-ray irradiation on bacteria. Gold Bull. 2008; 41(2):187–194.
182. Huang WC, Tsai PJ, Chen YC. Functional gold nanoparticles as photothermal agents for selective-killing of pathogenic bacteria. Nanomedicine (Lond.). 2007; 2(6):777–787. [PubMed: 18095845]
183. Gil-Tomás J, Tubby S, Parkin IP, et al. Lethal photosensitisation of *Staphylococcus aureus* using a toluidine blue O-tiopronin-gold nanoparticle conjugate. J. Mater. Chem. 2007; 17:3739–3746.
184. Perni S, Piccirillo C, Pratten J, et al. The antimicrobial properties of light-activated polymers containing methylene blue and gold nanoparticles. Biomaterials. 2009; 30(1):89–93. [PubMed: 18838166]
185. Hongwei G, Ho PL, Edmond T, Ling W, Bing X. Presenting vancomycin on nanoparticles to enhance antimicrobial activities. Nano Lett. 2003; 3(9):1261–1263.

186. Nath S, Kaittanis C, Tinkham A, Perez JM. Dextran-coated gold nanoparticles for the assessment of antimicrobial susceptibility. Anal. Chem. 2008; 80(4):1033–1038. [PubMed: 18198893]

187. Burygin GL, Khlebtsov BN, Shantrokha AN, Dykman LA, Bogatyrev VA, Khlebtsov NG. On the enhanced antibacterial activity of antibiotics mixed with gold nanoparticles. Nanoscale Res. Lett. 2009; 4(8):794–801. [PubMed: 20596384]

188. Nirmala Grace A, Pandian K. Antibacterial efficacy of aminoglycosidic antibiotics protected gold nanoparticles – a brief study. Colloids Surf. A Physicochem. Eng. Asp. 2007; 297(1):63–70.

189. Rai A, Prabhune A, Perry CC. Antibiotic mediated synthesis of gold nanoparticles with potent antimicrobial activity and their application in antimicrobial coatings. J. Mater. Chem. 2010; 20:6789–6798.

190. Chamundeeswari M, Sobhana SS, Jacob JP, et al. Preparation, characterization and evaluation of a biopolymeric gold nanocomposite with antimicrobial activity. Biotechnol. Appl. Biochem. 2010; 55(1):29–35. [PubMed: 19929854]

191. Khan S, Alam F, Azam A, Khan AU. Gold nanoparticles enhance methylene blue-induced photodynamic therapy: a novel therapeutic approach to inhibit *Candida albicans* biofilm. Int. J. Nanomedicine. 2012; 7:3245–3257. [PubMed: 22802686]

192. Di Gianvincenzo P, Marradi M, Martinez-Avila OM, Bedoya LM, Alcami J, Penades S. Gold nanoparticles capped with sulfate-ended ligands as anti-HIV agents. Bioorg. Med. Chem. Lett. 2010; 20(9):2718–2721. [PubMed: 20382017]

193. Lara HH, Ayala-Nunez NV, Ixtepan-Turrent L, Rodriguez-Padilla C. Mode of antiviral action of silver nanoparticles against HIV-1. J. Nanobiotechnol. 2010; 8:1.

194. Ravishankar Rai, V.; Jamuna Bai, A. Nanoparticles and their potential application as antimicrobials. In: Méndez-Vilas, A., editor. Science Against Microbial Pathogens: Communicating Current Research And Technological Advances. Badajoz, Spain: Formatex Research Center; 2011. p. 197-209.

195. Gupta A, Silver S. Silver as a biocide: will resistance become a problem? Nat. Biotechnol. 1998; 16(10):888. [PubMed: 9788326]

196. Matsumura Y, Yoshikata K, Kunisaki S, Tsuchido T. Mode of bactericidal action of silver zeolite and its comparison with that of silver nitrate. Appl. Environ. Microbiol. 2003; 69(7):4278–4281. [PubMed: 12839814]

197. Gogoi SK, Gopinath P, Paul A, Ramesh A, Ghosh SS, Chattopadhyay A. Green fluorescent protein-expressing *Escherichia coli* as a model system for investigating the antimicrobial activities of silver nanoparticles. Langmuir. 2006; 22(22):9322–9328. [PubMed: 17042548]

198. Smetana AB, Klabunde KJ, Marchin GR, Sorensen CM. Biocidal activity of nanocrystalline silver powders and particles. Langmuir. 2008; 24(14):7457–7464. [PubMed: 18543995]

199. Shrivastava S, Bera T, Roy A, Singh G, Ramachandrarao P, Dash D. Characterization of enhanced antibacterial effects of novel silver nanoparticles. Nanotech. 2007; 18(22):225103.

200. Holt KB, Bard AJ. Interaction of silveRI) ions with the respiratory chain of *Escherichia coli* : an electrochemical and scanning electrochemical microscopy study of the antimicrobial mechanism of micromolar Ag^{+} . Biochemistry. 2005; 44(39):13214–13223. [PubMed: 16185089]

201. Dibrov P, Dzioba J, Gosink KK, Hase CC. Chemiosmotic mechanism of antimicrobial activity of $Ag(^{+})$ in *Vibrio cholerae*. Antimicrob. Agents Chemother. 2002; 46(8):2668–2670. [PubMed: 12121953]

202. Sondi I, Salopek-Sondi B. Silver nanoparticles as antimicrobial agent: a case study on *E. coli* as a model for Gram-negative bacteria. J. Colloid. Interface Sci. 2004; 275(1):177–182. [PubMed: 15158396]

203. Panacek A, Kvitek L, Prucek R, et al. Silver colloid nanoparticles: synthesis, characterization, and their antibacterial activity. J. Phys. Chem. B. 2006; 110(33):16248–16253. [PubMed: 16913750]

204. Cho KH, Park JE, Osaka T, Park SG. The study of antimicrobial activity and preservative effects of nanosilver ingredient. Electrochim. Acta. 2005; 51(5):956–960.

205. Baker C, Pradhan A, Pakstis L, Pochan DJ, Shah SI. Synthesis and antibacterial properties of silver nanoparticles. J. Nanosci. Nanotechnol. 2005; 5(2):244–249. [PubMed: 15853142]

206. Martinez-Castanon GA, Nino-Martinez N, Martinez-Gutierrez F, Martinez-Mendoza JR, Ruiz F. Synthesis and antibacterial activity of silver nanoparticles with different sizes. J. Nanopart. Res. 2008; 10(8):1343–1348.

207. Pal S, Tak YK, Song JM. Does the antibacterial activity of silver nanoparticles depend on the shape of the nanoparticle? A study of the Gram-negative bacterium Escherichia coli. Appl. Environ. Microbiol. 2007; 73(6):1712–1720. [PubMed: 17261510]

208. Brett DW. A discussion of silver as an antimicrobial agent: alleviating the confusion. Ostomy Wound Manage. 2006; 52(1):34–41. [PubMed: 16464989]

209. Hernandez-Sierra JF, Ruiz F, Pena DC, et al. The antimicrobial sensitivity of *Streptococcus mutans* to nanoparticles of silver, zinc oxide, and gold. Nanomedicine. 2008; 4(3):237–240. [PubMed: 18565800]

210. Besinis A, De Peralta T, Handy RD. The antibacterial effects of silver, titanium dioxide and silica dioxide nanoparticles compared with the dental disinfectant chlorhexidine on *Streptococcus mutans* using a suite of bioassays. Nanotoxicology. 2014; 8(1):1–16. [PubMed: 23092443]

211. Feng QL, Wu J, Chen GQ, Cui FZ, Kim TN, Kim JO. A mechanistic study of the antibacterial effect of silver ions on *Escherichia coli* and *Staphylococcus aureus*. J. Biomed. Mater. Res. 2000; 52(4):662–668. [PubMed: 11033548]

212. Jung WK, Koo HC, Kim KW, Shin S, Kim SH, Park YH. Antibacterial activity and mechanism of action of the silver ion in *Staphylococcus* aureus and *Escherichia coli*. Appl. Environ. Microbiol. 2008; 74(7):2171–2178. [PubMed: 18245232]

213. Aymonier C, Schlotterbeck U, Antonietti L, et al. Hybrids of silver nanoparticles with amphiphilic hyperbranched macromolecules exhibiting antimicrobial properties. Chem. Commun. (Camb.). 2002; (24):3018–3019. [PubMed: 12536795]

214. Melaiye A, Sun Z, Hindi K, et al. Silve(I)-imidazole cyclophane gem-diol complexes encapsulated by electrospun tecophilic nanofibers: formation of nanosilver particles and antimicrobial activity. J. Am. Chem. Soc. 2005; 127(7):2285–2291. [PubMed: 15713108]

215. Banerjee M, Mallick S, Paul A, Chattopadhyay A, Ghosh SS. Heightened reactive oxygen species generation in the antimicrobial activity of a three component iodinated chitosan-silver nanoparticle composite. Langmuir. 2010; 26(8):5901–5908. [PubMed: 20085297]

216. Lok CN, Ho CM, Chen R, et al. Proteomic analysis of the mode of antibacterial action of silver nanoparticles. J. Proteome Res. 2006; 5(4):916–924. [PubMed: 16602699]

217. Otani M, Tabata J, Ueki T, Sano K, Inouye S. Heat-shock-induced proteins from *Myxococcus xanthus*. J. Bacteriol. 2001; 183(21):6282–6287. [PubMed: 11591671]

218. Kitagawa M, Matsumura Y, Tsuchido T. Small heat shock proteins, IbpA and IbpB, are involved in resistances to heat and superoxide stresses in *Escherichia coli*. FEMS Microbiol. Lett. 2000; 184(2):165–171. [PubMed: 10713416]

219. Nanda A, Saravanan M. Biosynthesis of silver nanoparticles from *Staphylococcus aureus* and its antimicrobial activity against MRSA and MRSE. Nanomedicine. 2009; 5(4):452–456. [PubMed: 19523420]

220. Brown AN, Smith K, Samuels TA, Lu J, Obare SO, Scott ME. Nanoparticles functionalized with ampicillin destroy multiple-antibiotic-resistant isolates of *Pseudomonas aeruginosa* and *Enterobacter aerogenes* and methicillin-resistant *Staphylococcus aureus*. Appl. Environ. Microbiol. 2012; 78(8):2768–2774. [PubMed: 22286985]

221. Baram-Pinto D, Shukla S, Perkas N, Gedanken A, Sarid R. Inhibition of herpes simplex virus type 1 infection by silver nanoparticles capped with mercaptoethane sulfonate. Bioconjug. Chem. 2009; 20(8):1497–1502. [PubMed: 21141805]

222. Lu L, Sun RW, Chen R, et al. Silver nanoparticles inhibit hepatitis B virus replication. Antivir. Ther. 2008; 13(2):253–262. [PubMed: 18505176]

223. Sun L, Singh AK, Vig K, Pillai SR, Singh SR. Silver nanoparticles inhibit replication of respiratory syncytial virus. J. Biomed. Nanotech. 2008; 4(2):149–158.

224. Rogers JV, Parkinson CV, Choi YW, Speshock JL, Hussain SM. A preliminary assessment of silver nanoparticle inhibition of monkeypox virus plaque formation. Nanoscale Res. Lett. 2008; 3(4):129–133.

225. Kim KJ, Sung WS, Moon SK, Choi JS, Kim JG, Lee DG. Antifungal effect of silver nanoparticles on dermatophytes. J. Microbiol. Biotechnol. 2008; 18(8):1482–1484. [PubMed: 18756112]

226. Kim KJ, Sung WS, Suh BK, et al. Antifungal activity and mode of action of silver nano-particles on *Candida albicans*. Biometals. 2009; 22(2):235–242. [PubMed: 18769871]

227. Gajbhiye M, Kesharwani J, Ingle A, Gade A, Rai M. Fungus-mediated synthesis of silver nanoparticles and their activity against pathogenic fungi in combination with fluconazole. Nanomedicine. 2009; 5(4):382–386. [PubMed: 19616127]

228. Couleaud P, Morosini V, Frochot C, Richeter S, Raehm L, Durand JO. Silica-based nanoparticles for photodynamic therapy applications. Nanoscale. 2010; 2(7):1083–1095. [PubMed: 20648332]

229. Walter WG, Stober A. Probe method for the microbial sampling of hospital carpets. Health Lab. Sci. 1968; 5(3):162–170. [PubMed: 5671179]

230. Brevet D, Gary-Bobo M, Raehm L, et al. Mannose-targeted mesoporous silica nanoparticles for photodynamic therapy. Chem. Commun. (Camb.). 2009; (12):1475–1477. [PubMed: 19277361]

231. Cheng Y, CS A, Meyers JD, Panagopoulos I, Fei B, Burda C. Highly efficient drug delivery with gold nanoparticle vectors for *in vivo* photodynamic therapy of cancer. J. Am. Chem. Soc. 2008; 130(32):10643–10647. [PubMed: 18642918]

232. Carpenter AW, Worley BV, Slomberg DL, Schoenfisch MH. Dual action antimicrobials: nitric oxide release from quaternary ammonium-functionalized silica nanoparticles. Biomacromolecules. 2012; 13(10):3334–3342. [PubMed: 22998760]

233. Tassa C, Shaw SY, Weissleder R. Dextran-coated iron oxide nanoparticles: a versatile platform for targeted molecular imaging, molecular diagnostics, and therapy. Acc. Chem. Res. 2011; 44(10):842–852. [PubMed: 21661727]

234. Mccarthy JR, Kelly KA, Sun EY, Weissleder R. Targeted delivery of multifunctional magnetic nanoparticles. Nanomedicine (Lond.). 2007; 2(2):153–167. [PubMed: 17716118]

235. Choi KH, Lee HJ, Park BJ, et al. Photosensitizer and vancomycin-conjugated novel multifunctional magnetic particles as photoinactivation agents for selective killing of pathogenic bacteria. Chem. Commun. (Camb.). 2012; 48(38):4591–4593. [PubMed: 22473513]

236. Lim ME, Lee YL, Zhang Y, Chu JJ. Photodynamic inactivation of viruses using upconversion nanoparticles. Biomaterials. 2012; 33(6):1912–1920. [PubMed: 22153019]

237. Wainwright M. Local treatment of viral disease using photodynamic therapy. Int. J. Antimicrob. Agents. 2003; 21(6):510–520. [PubMed: 12791463]

238. Haase M, Schafer H. Upconverting nanoparticles. Angew. Chem. Int. Ed. Engl. 2011; 50(26): 5808–5829. [PubMed: 21626614]

239. Feynman RP. There's plenty of room at the bottom. Eng. Sci. 1960; 23(5):22–36.

240. Von Tappeiner H. Uber die Wirkung fluoreszierender Stoffe auf Infusorien nach Versuchen von O. Raab. Muench. Med. Wochenschr. 1900; 47(5)

241. Kharkwal GB, Sharma SK, Huang YY, Dai T, Hamblin MR. Photodynamic therapy for infections: clinical applications. Lasers Surg. Med. 2011; 43(7):755–767. [PubMed: 22057503]

242. Etheridge ML, Campbell SA, Erdman AG, Haynes CL, Wolf SM, Mccullough J. The big picture on nanomedicine: the state of investigational and approved nanomedicine products. Nanomedicine. 2013; 9(1):1–14. [PubMed: 22684017]

Executive summary

- Photodynamic inactivation uses nontoxic dyes and harmless visible light to kill all known micro-organisms regardless of antibiotic resistance.
- Singlet oxygen is formed via type 2 photochemical pathway and reactive oxygen species and radicals via type 1 photochemical pathway.
- Many photosensitizers are insoluble and tend to aggregate, and nanoparticle-based delivery vehicles can improve their performance.
- Photostable titanium dioxide nanoparticles mediate photocatalysis and can produce self-sterilizing surfaces.
- Carbon nanostructures such as fullerenes, nanotubes and graphene can be photoactivated to kill microbes.
- Gold and silver nanoparticles can potentiate photodynamic inactivation via a plasmon-resonance effect.
- Naturally occurring polymers such as chitosan and cellulose can be used to produce nontoxic photoactivated nanomedicines.
- Rare earth mineral nanoparticles can be used to transduce near-infrared light into short wavelength visible light for better tissue penetration and photosensitizer excitation.

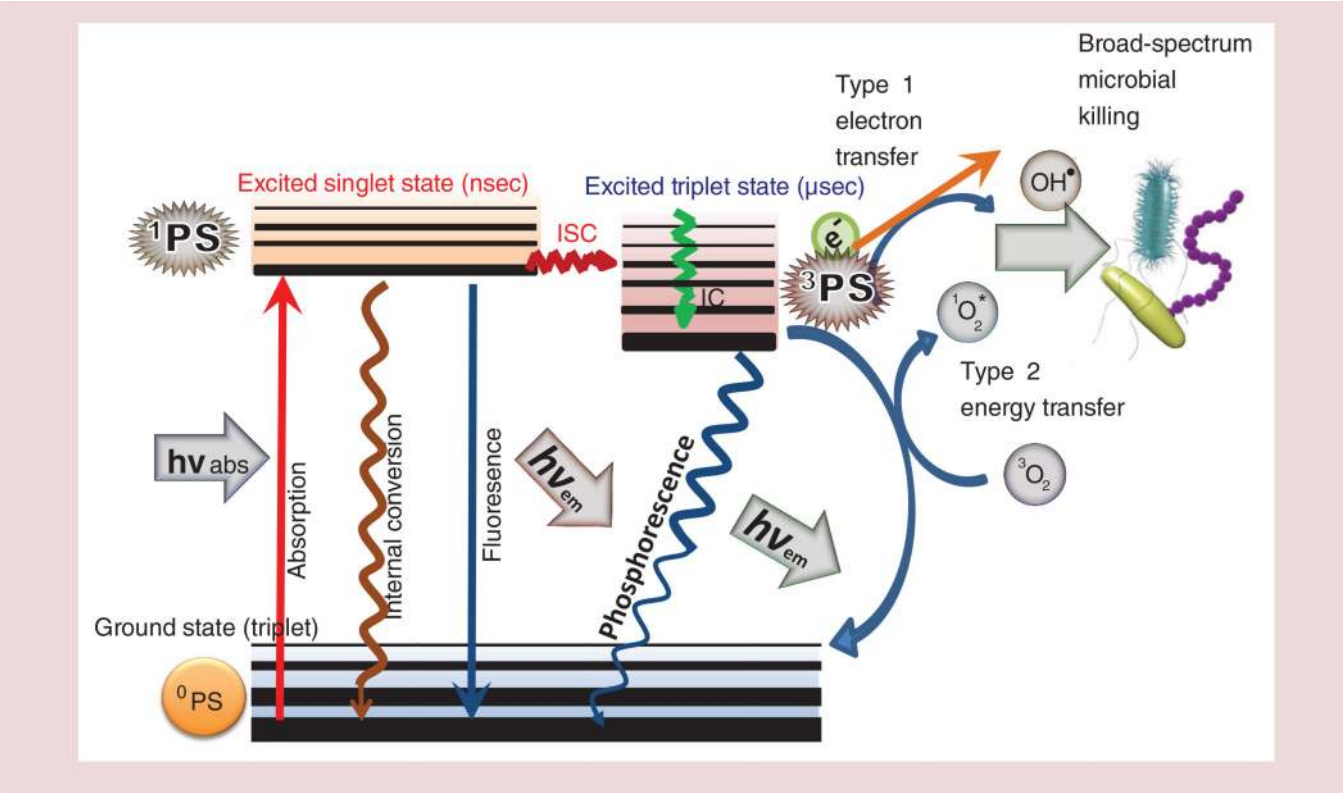

Figure 1. Jablonski diagram

Ground state photosensitizer (^{0}PS) absorbs light to form first excited singlet state (^{1}PS) that (in addition to losing energy by fluorescence or conversion to heat) undergoes intersystem crossing to form the long lived first excited triplet state (^{3}PS). The triplet state can undergo type 1 (electron transfer) photochemical reaction to form superoxide and hydroxyl radical, and/or type 2 (energy transfer) photochemical reaction to form singlet oxygen. These ROS can oxidatively damage and kill all known forms of microorganism.

$h\nu_{abs}$: Absorbed light; $h\nu_{em}$: Emitted light; IC: Internal conversion; ISC: Intersyetem crossing; ROS: Reactive oxygen species; PS: Photosensitizer.

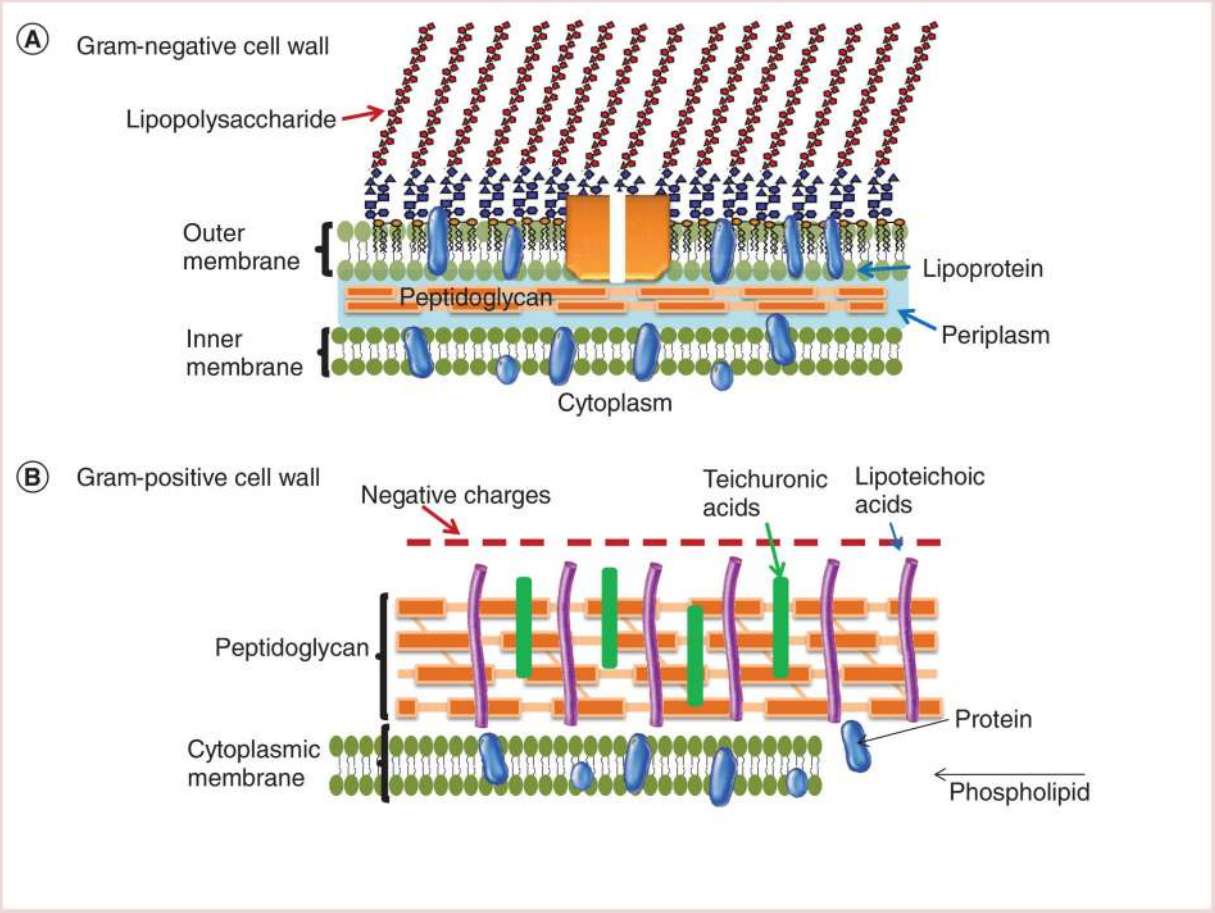

Figure 2. Gram-positive and Gram-negative cell walls

(A) Gram-negative bacteria have a double lipid bilayer (inner and outer membrane) separated by periplasm and peptidoglycan. The outer membrane contains porins and lipoproteins and is decorated with lipopolysaccharide chains with a negative charge. **(B)** Gram-positive bacteria have a single lipid bilayer surrounded by a thick but porous layer of peptidoglycan, with teichuronic and lipoteichoic acids providing a negative charge.

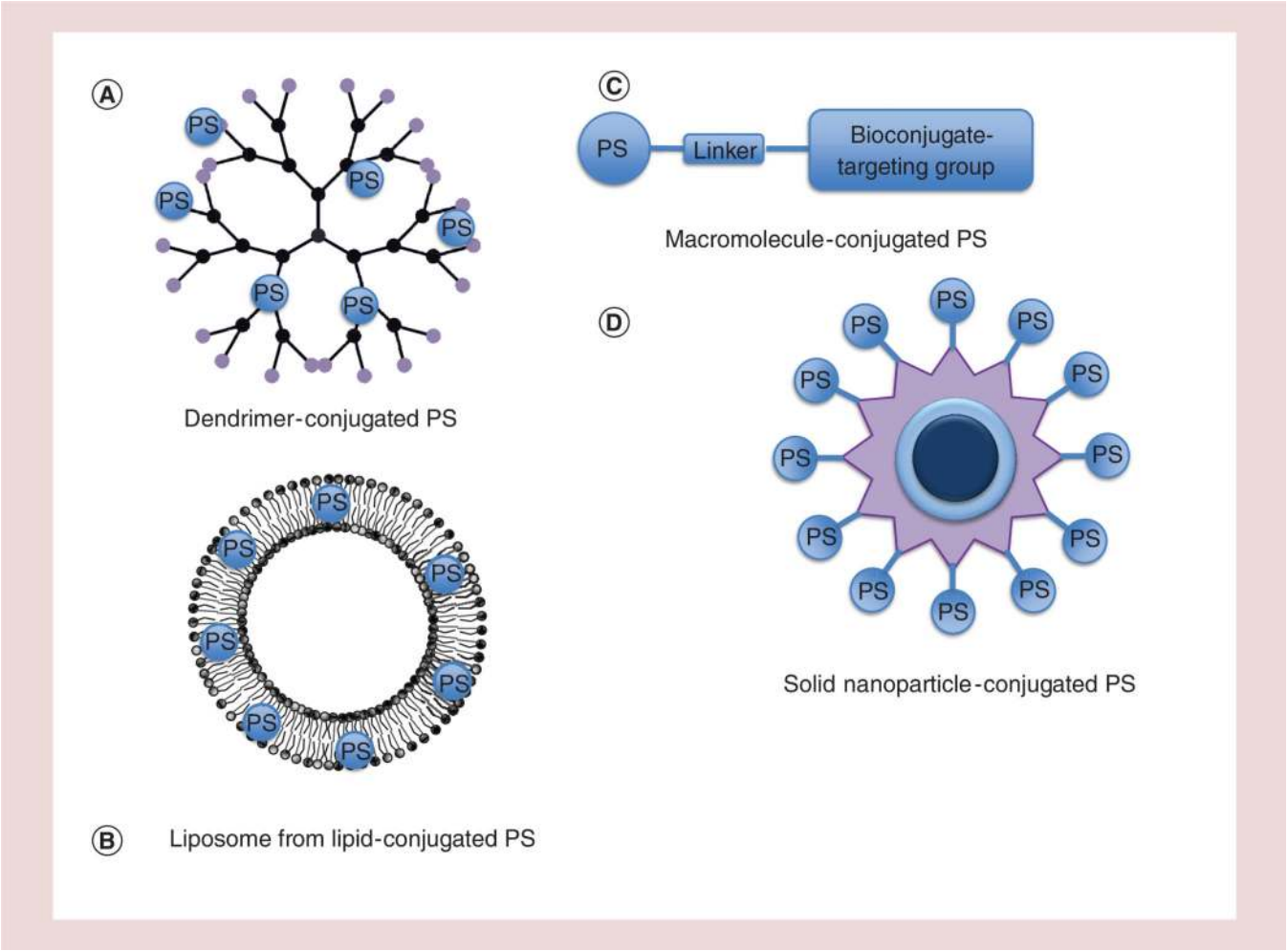

Figure 3. Nanoparticles that have been covalently modified with photosensitizers

(A) Dendrimers conjugated to PS. **(B)** Macromolecules with biotargeting properties such as antibodies. **(C)** Lipid-conjugated PS self-assemble into liposomes. **(D)** Solid nanoparticles can be conjugated to PS.

PS: Photosensitizer.

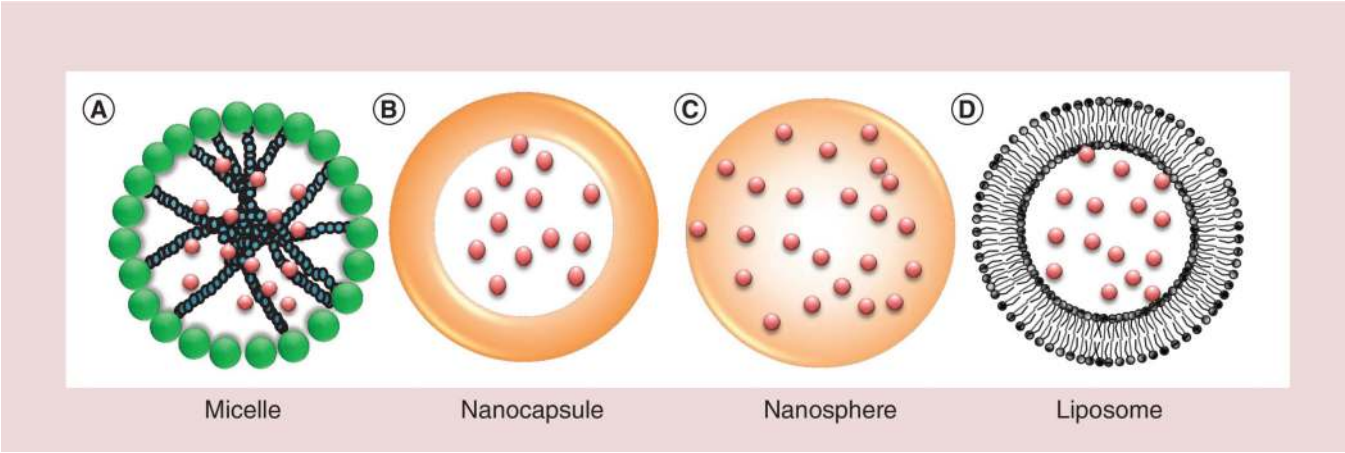

Figure 4. Noncovalent encapsulation of photosensitizers

Polymeric nanoparticles are sub-μm colloidal particles designed to solubilize hydrophobic photosensitizer. They include: **(A)** nanomicelles in which amphiphilic copolymers with hydrophobic and hydrophilic blocks self-assemble to entrap the cargo; **(B)** nanocapsules, in which the cargo is in solution and surrounded by a shell-like wall; **(C)** nanospheres, in which the cargo is dissolved, adsorbed or dispersed throughout the matrix, attached to the surface or attached to the polymer matrix; and **(D)** liposomes in which an amphiphlic polymer self-assembles into a lipid bilayer that forms a unilamellar vesicle that encapsulates the cargo [50].

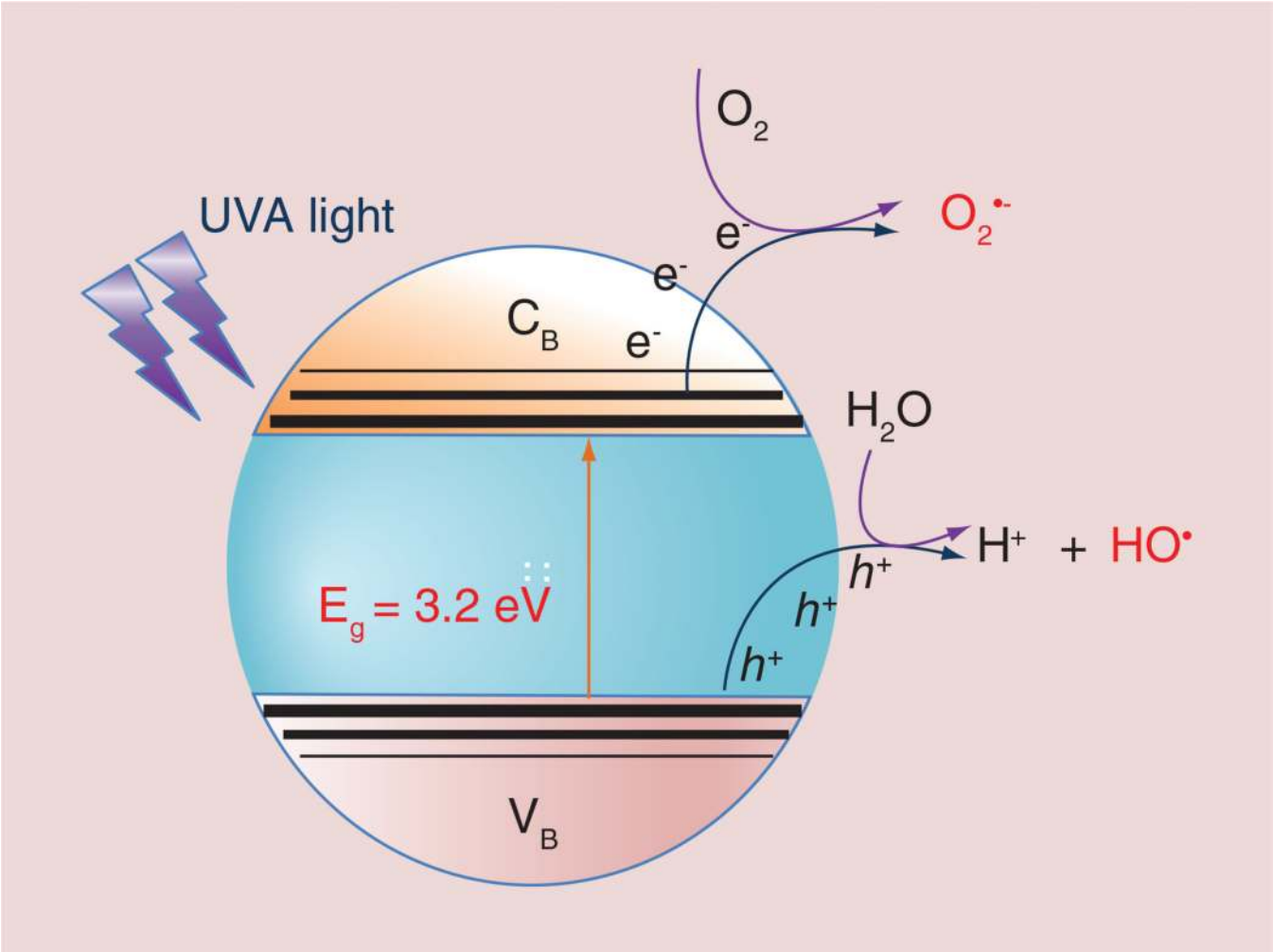

Figure 5. Titania photocatalysis

Schematic illustration of main processes in the photocatalytic reaction of TiO_2. Nanoparticles have a sufficiently large surface area to allow this process to be efficient. Electrons are excited by UVA light from the semiconductor valence band to the conductance band. The electrons in the conductance band undergo electron transfer to oxygen to form superoxide, and the holes in the valence band react with water to form hydroxyl radicals. The ROS produced ($O2^{\cdot-}$ and $HO^{\cdot}$) can kill microorganisms.

C_B: Conduction band; E_g: Energy gap; UVA: Ultraviolet A; V_B: Valence band.

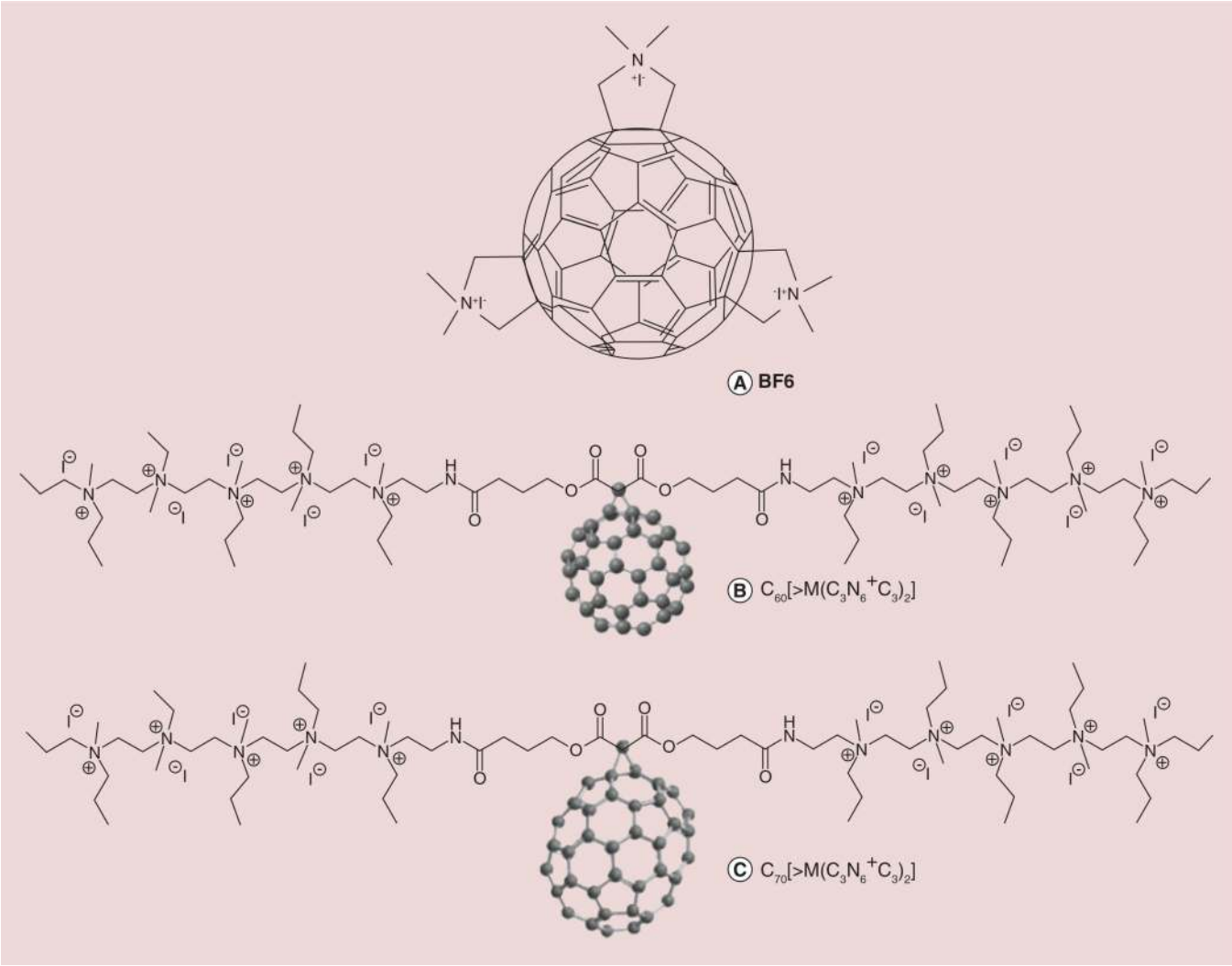

Figure 6. Fullerenes used in antimicrobial photodynamic therapy

(A) The tri-cationic C60 fullerene BF6. **(B)** The deca-cationic C60 fullerene, $C60[>M(C_3N_6{}^+C_3)_2]$. **(C)** The deca-cationic C70 fullerene, $C70[>M(C_3N_6{}^+C_3)_2]$.

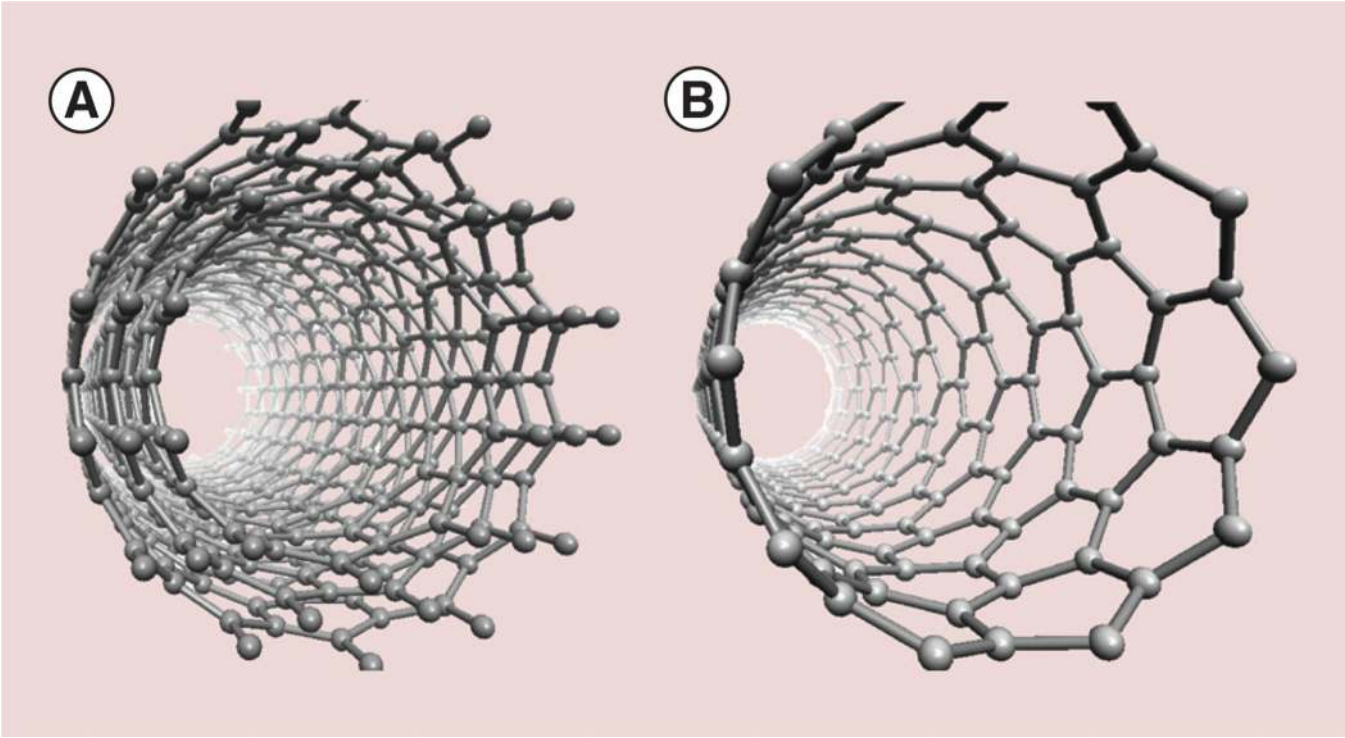

Figure 7. Carbon nanotubes

(A) Multiwalled carbon nanotubes. **(B)** Single-walled arbon nanotubes.

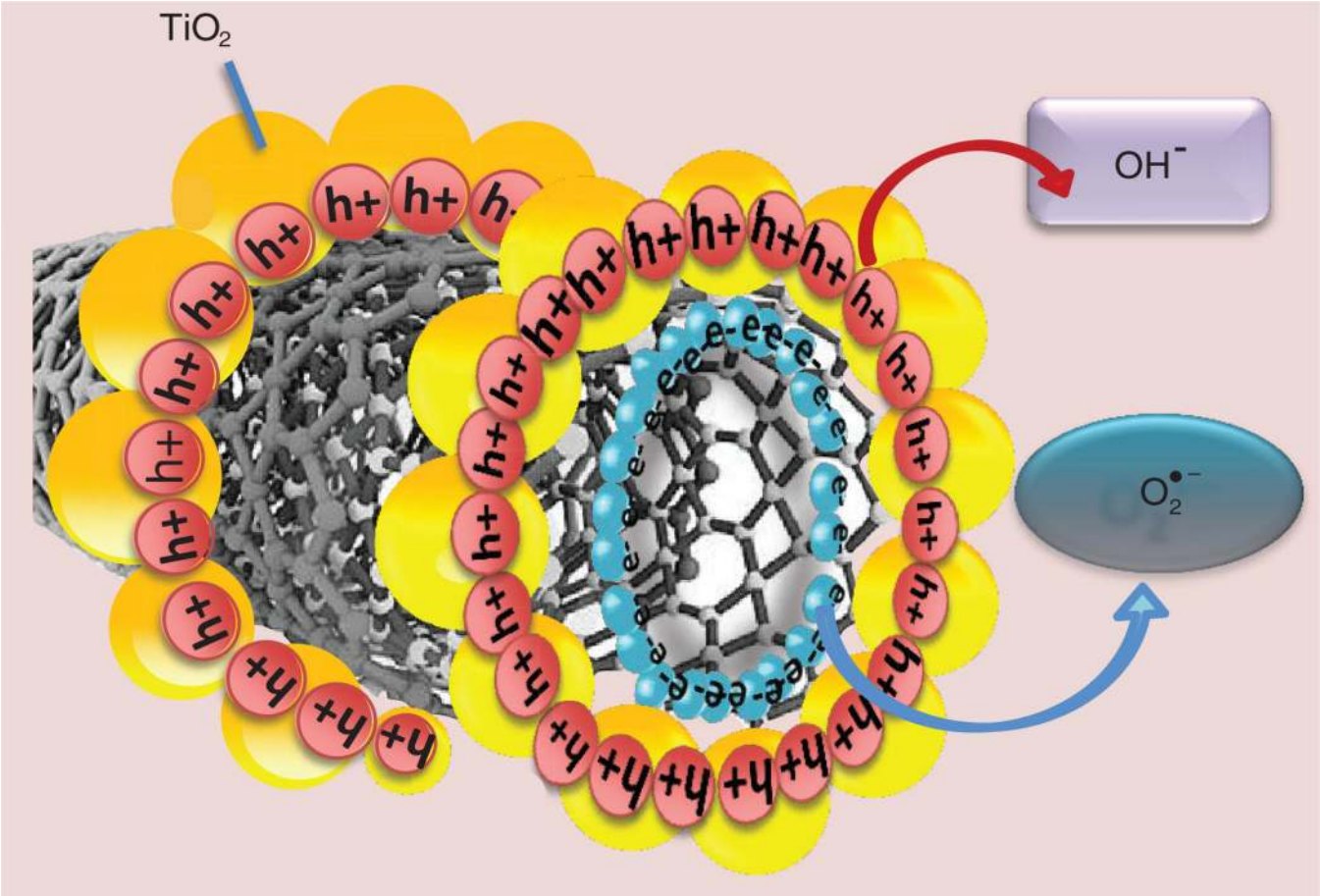

Figure 8. Titanium dioxide coated carbon nanotubes

The vertical array of multiwalled carbon nanotubes acts as a filter for bacterial retention while TiO_2 acts as a bactericidal photocatalyst.

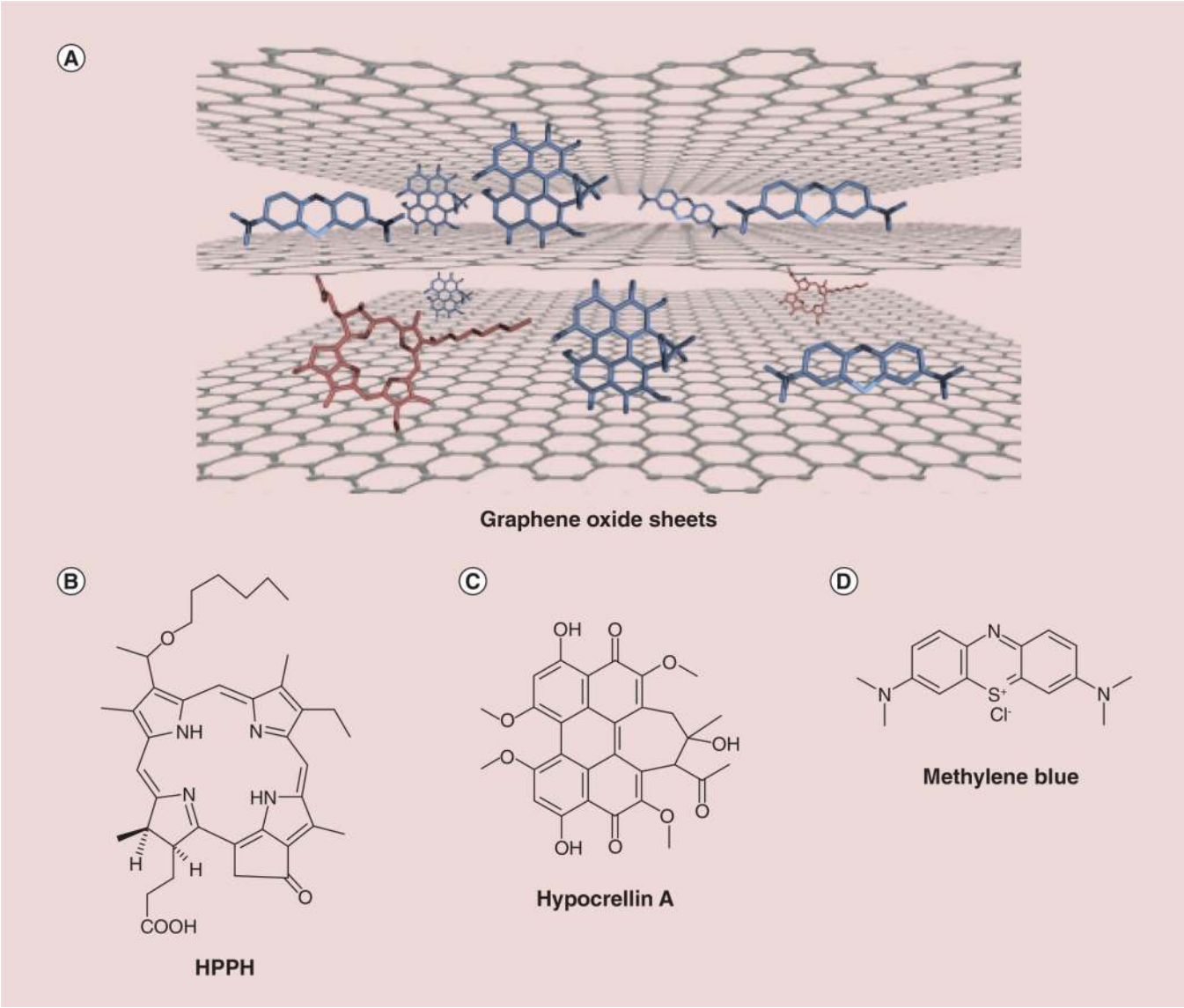

Figure 9. Graphene-loaded photosensitizers

(A) Hydrophobic photosensitizer can be 'sandwiched' between graphene sheets by π–π stacking. Examples of photosensitizer that have been loaded on to graphene are: **(B)** HPPH; **(C)** hypocrellin a; **(D)** methylene blue.

HPPH: 2-(1-Hexyloxyethyl)-2-devinyl pyropheophorbide-a.

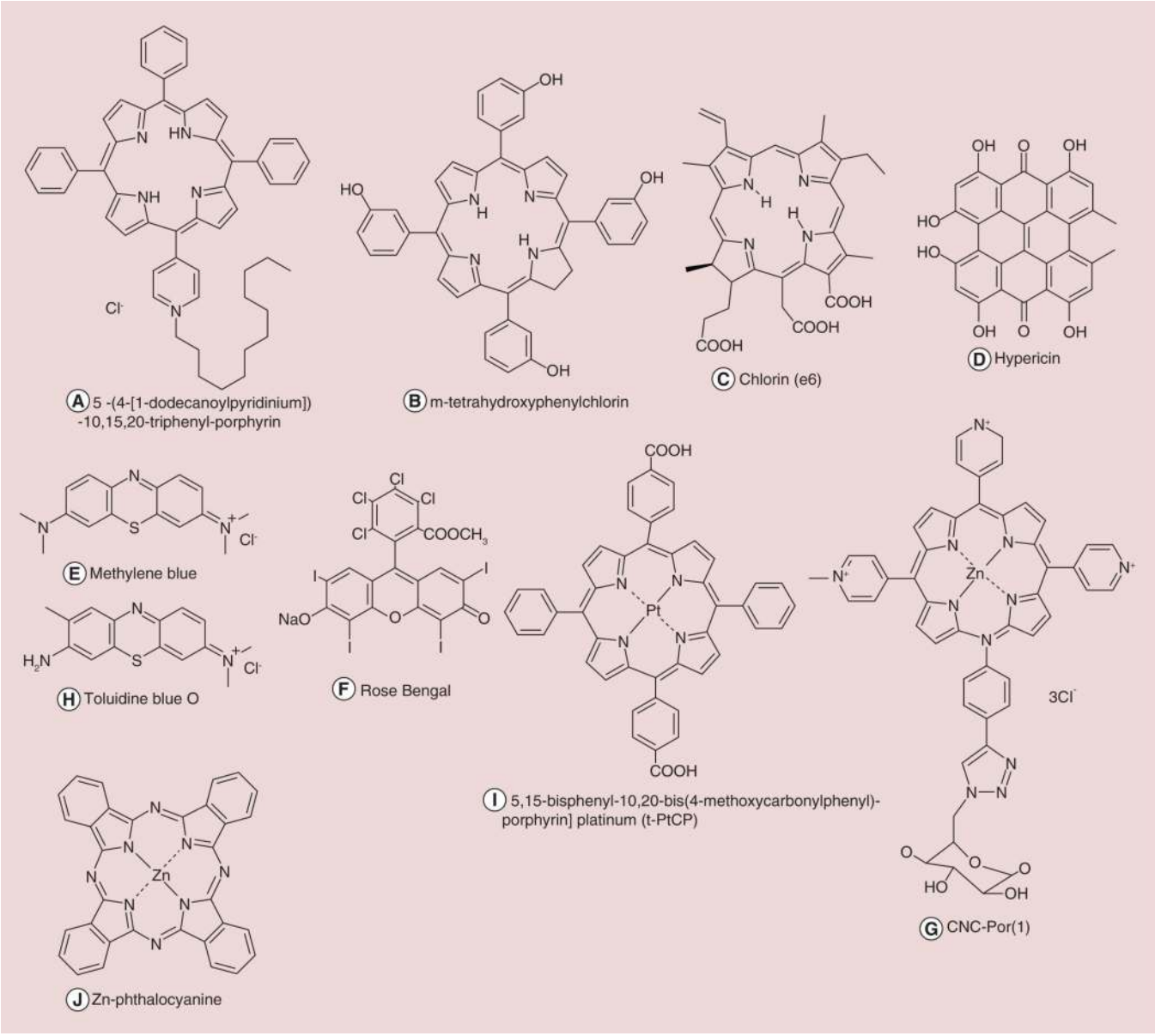

Figure 10. Chemical structure of antimicrobial photosensitizers

(A) 5-[4-(1-dodecanoylpyridinium)]-10,15,20-triphenyl-porphyrin; **(B)** m-tetrahydroxyphenyl-chlorin; **(C)** chlorin(e6); **(D)** hypericin; **(E)** methylene blue; **(F)** Rose Bengal; **(G)** CNC-Por(1); **(H)** toluidine blue O; **(I)** 5,15-bisphenyl-10,20-bis(4-methoxycarbonylphenyl)- porphyrin] platinum (t-PtCP); **(J)** Zn-phthalocyanine.

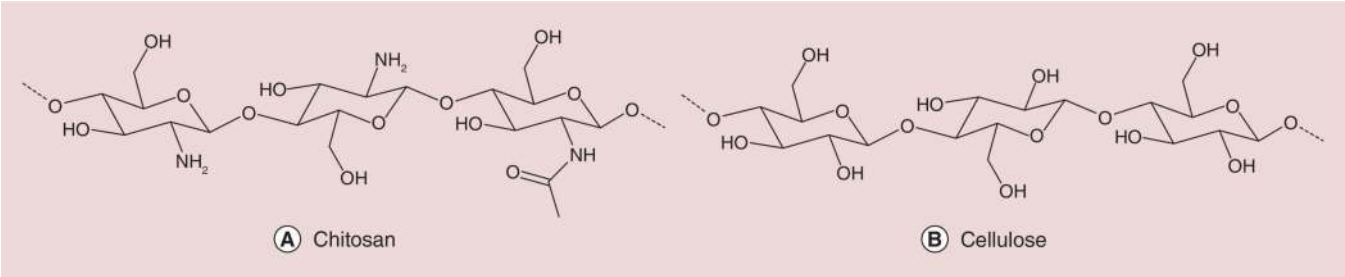

Figure 11. Naturally occurring biopolymers used to form nanoparticles
(A) Chitosan. **(B)** Cellullose.

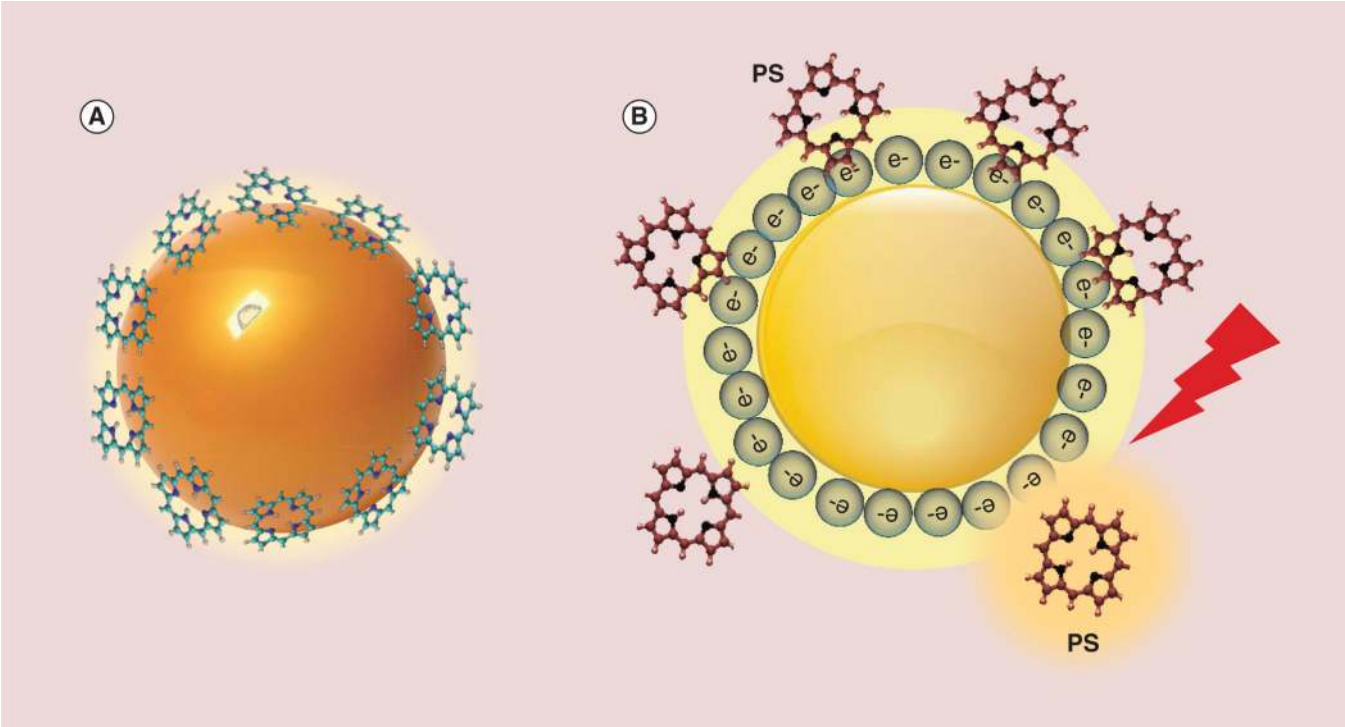

Figure 12. Gold nanoparticle-conjugated photosensitizer

(A) Gold nanoshell encapsulating a PS. **(B)** Plasmonic gold nanoparticle. The local electric field caused by conductance electrons potentiates the optical field close to the surface and increases the fluorescence or photoactivity of an attached PS.

PS: Photosensitizer.

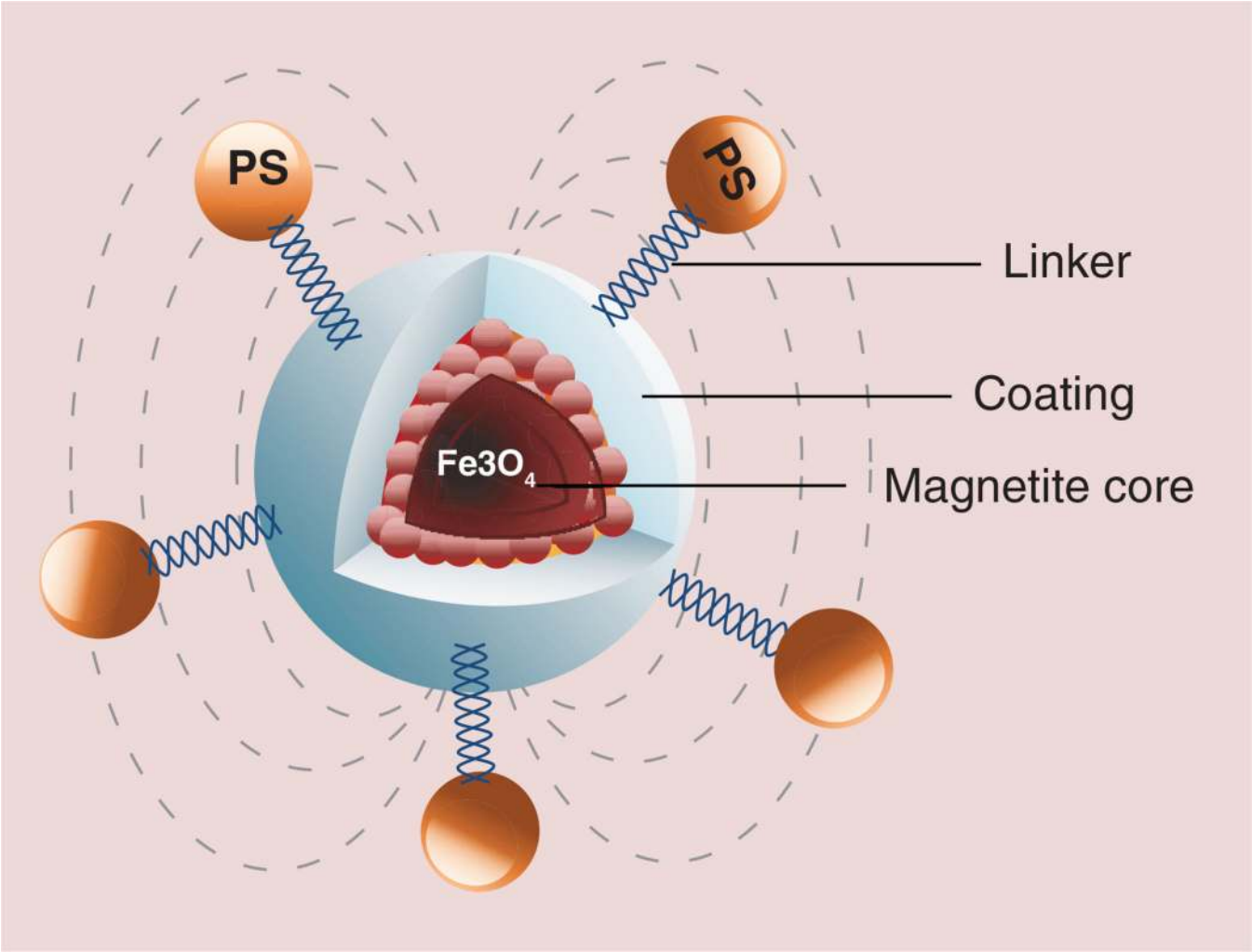

Figure 13. Magnetic nanoparticle-conjugated photosensitizer

Consists of a magnetite core (Fe_3O_4) coated by a biologically compatible layer such as PEG, and the PS are covalently attached by flexible linkers.

PS: Photosensitizer.

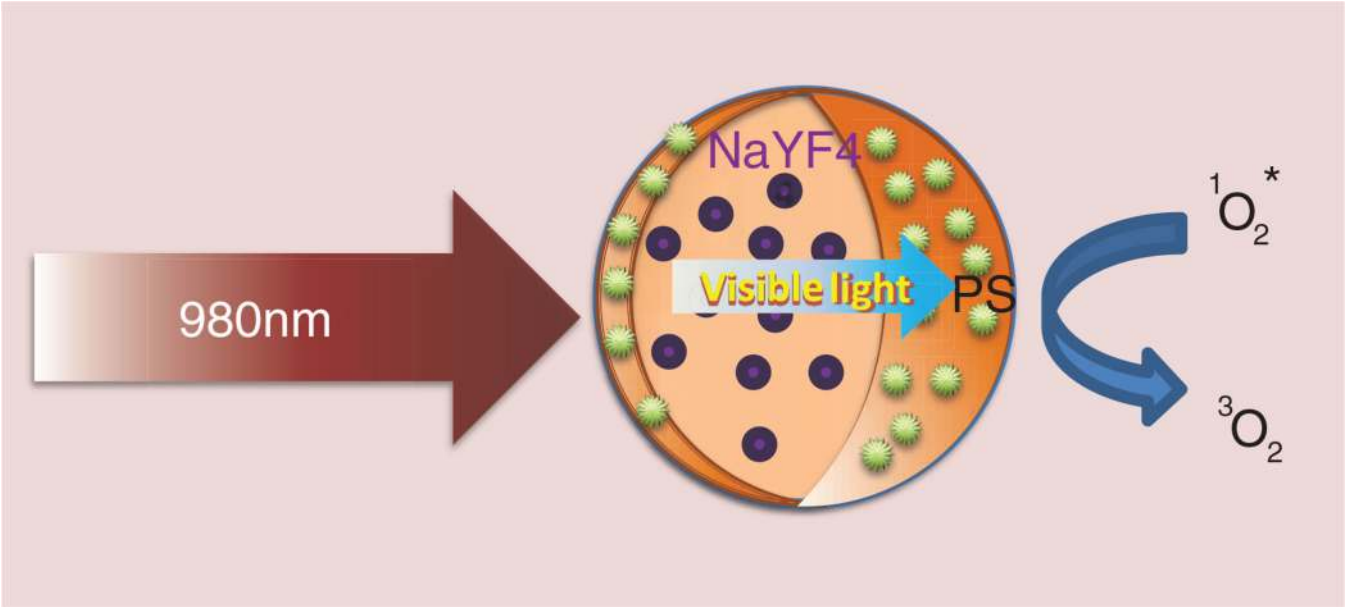

Figure 14. Upconverting nanoparticle-mediated photodynamic therapy

Nanoparticles made of rare earth salts such as NaYF4 absorb continuous wavelength 980-nm light and emit 490-nm light that can excite a conjugated PS.

PS: Photosensitizer.

Table 1

Examples of Gram-negative and Gram-positive bacteria shown to be killed by TiO_2 photocatalytic disinfection.

Organism	Notes	Ref.
Acinetobacter	TiO_2 suspension	[60]
Acinetobacter baumanii	Carbon-doped TiO_2	[61]
Escherichia coli	WO_3 nanoparticle-doped TiO_2	[62]
E. coli	Degussa P25 impregnated cloth filter	[63]
E. coli	ZnO nanorods employed with glass substrate	[64]
E.coli ATCC 13706	Degussa P25 immobilized on glass substrate	[65]
E. coli ATCC 10536	Ag and CuO–TiO_2 hybrid catalysts	[66]
E. coli IM303	TiO_2 coated air filter	[67]
Pseudomonas aeruginosa	Surfaces	[68]
P. aeruginosa	Coated Al fibers	[69]
P. aeruginosa	Catheters	[70]
Serratia marcescens	Degussa P25 suspension	[71] [72]
Shigella flexneri	C-doped TiO_2	[61]
Vibrio vulnificus	TiO_2-impregnated steel fibers for water treatment	[73]
Bacillus cereus, B. cereus spores	TiO_2 suspension TiO_2 suspension	[74] [75]
Clostridium perfringens spores NCIMB 6125	TiO_2 film on metal electrode Degussa P-25 + UVC	[76]
C. perfringens spores		[77]
Enterococcus faecalis CECT 481	Immobilized TiO_2 Degussa P25 suspension	[78] [79]
MRSA	Fe_3O_4–TiO_2core/shell magnetic nanoparticles in suspension	[80]

MRSA TiO_2 thin film on titanium [81].

MRSA: Methicillin-resistant *Staphylococcus aureus*; UVC: Ultraviolet C.

Table 2

Examples of fungi, protozoa and algae shown to be killed by TiO_2 photocatalytic disinfection.

Organism	Notes	Ref.
Aspergillus niger AS3315	Wood coated with TiO_2	[82]
A. niger spores	Degussa P25 film on quartz discs	[83]
A. niger	Thin films of TiO_2 on glass plates	[84]
Candida albicans	TiO_2-coated surfaces	[68]
Acanthamoeba castellanii	Degussa P25 suspension	[85]
Cryptosporidium parvum	UVC + TiO_2	[86]

UVC: Ultraviolet C.

Table 3

Viruses shown to be inactivated by TiO_2 photocatalytic disinfection.

Host	Virus	Ref.
Birds	Influenza (avian) A/H5N2	[87]
Human	Hepatitis B virus surface antigen HBsAg	[88]
Human	Influenza A/H1N1	[89]
Human	Influenza A/H3N2	[90]
Human	*Poliovirus* type 1 (ATCC VFR-192)	[91]
Human	SARS coronavirus	[92]